

## Review

# Recent progress on organic light-emitting diodes with phosphorescent ultrathin (<1nm) light-emitting layers

Yanqin Miao<sup>1,2,\*</sup> and Mengna Yin<sup>1</sup>

## SUMMARY

In recent years, phosphorescent dyes forming ultrathin light-emitting layers (<1 nm, UEMLs) have been widely applied to fabricate monochromatic and white organic light-emitting diodes (OLEDs) owing to its merits of simplified device structure and preparation process, more flexible design, lower material consumption, and complete exciton utilization. In addition, it was demonstrated that the OLEDs with UEMLs achieved high electroluminescence performance comparable to the conventional doping-based devices. Structurally, OLEDs were structured with phosphorescent UEMLs inserted into nonluminous materials, heterojunction interface as well as into luminescent materials including phosphorescent, conventional fluorescent, thermally activated delayed fluorescence, and exciplex emitters. We carefully reviewed the successful applications of UEMLs in OLEDs and underlying working mechanism of corresponding devices, and also emphasized the representative achievements about OLEDs with UEMLs, aimed at forming a comprehensive summary of the present research for UEMLs-based OLEDs. In the end, we also gave an outlook for the future development of UEMLs-based OLEDs.

## INTRODUCTION

Organic light-emitting diodes (OLEDs) are very promising for solid-state lighting and flat-panel displays fields because of their unique advantages such as self-luminous, surface light source, fast response, broad viewing angle, like-sunlight, thin thickness, transparent, as well as flexibility (Reineke et al., 2009; Gather et al., 2011; Byeon et al., 2019; Yin et al., 2019; Pode, 2020). In conventional fluorescent OLEDs, only singlet excitons contribute to photon emission, which make the devices present rather limited efficiency. By contrast, phosphorescent OLEDs can achieve 100% internal quantum efficiency (IQE) and subsequently obtain higher device efficiency owing to the complete utilization of singlet and triplet excitons (Yang et al., 2015; Kim et al., 2014; Lee et al., 2014a). In the last three decades, it was well demonstrated that a reasonable light-emitting layer (EML) is very critical to fulfill high device performance for phosphorescent OLEDs. (Han et al., 2021; D'Andrade et al., 2004; Sun et al., 2014; Miao et al., 2017a). Where, EMLs are usually built by adopting a host-guest system because such EMLs can effectively suppress the molecular aggregation and excitons quenching, contributing to higher device efficiency. Besides, such EMLs can also suppress device aging and increase flexibility in device design.(Liu et al., 2015; Miao et al., 2018a). However, the host-guest EMLs are generally prepared using the doping technology, which leads to more complicated device structure and fabrication process, especially for white OLEDs which usually require the introduction of two or more complementary emitters (Luo et al., 2019; Wang et al., 2014; Ying et al., 2020a). Limitations of doped-EMLs in the development of phosphorescent OLEDs are discussed in limitations of doped-EMLs in the development of OLEDs section.

Owing to the intrinsic nature of sub-monolayer, the introduction of ultrathin light-emitting layers (<1 nm, UEMLs) don't significantly affect the carrier behavior of devices. Hence, UEMLs were utilized as probe layer initially, and the approximate excitons distribution was obtained by varying the location of it and checking the electroluminescence (EL) spectra of corresponding devices (Tan et al., 2015; Tang et al., 2018; Miao et al., 2018b; Ma et al., 2014). Then, the structural characteristics of UEMLs are studied in-depth. It is found when the thickness of UEMLs is less than 1 nm, the molecules in UEMLs can be considered as guest doped in host materials on both sides, which can be called delta-doping (Zhao et al., 2011) ( $\delta$ -doping) and partially

---

<sup>1</sup>Key Laboratory of Interface Science and Engineering in Advanced Materials, Ministry of Education, Taiyuan University of Technology, Taiyuan, 030024, China

<sup>2</sup>Shanxi-Zheda Institute of Advanced Materials and Chemical Engineering, 030000, Taiyuan, 030024, China

\*Correspondence:  
miaoqyanqin@tyut.edu.cn  
<https://doi.org/10.1016/j.isci.2022.103804>



doped (Yang and Jabbour, 2013) methods. Because molecules forming UEMls are not in the form of a neat layer but partially penetrate the adjacent layers, which is beneficial for reducing molecular aggregation and eliminating concentration quenching. This has been proved from the atomic force microscopy images (AFM) where molecules of UEMls occupy the concave and convex sites of the surface for the bottom layer (Liu et al., 2014, 2016). Because the sizes of these emitters are normally smaller than 1 nm, these emitters are deposited with few islands on adjacent layers. The high resolution AFM images further show that the surface roughness increases when more molecules are deposited, indicating that such thin films are formed like islands (Zhao et al., 2018a; Meng et al., 2016). The molecules of UEMls can be considered to be doped in two-dimensional form, but the hosts and dopants in conventional doping methods are mixed in three-dimensional form. Therefore, UEMl is a special form of doping emitters without co-doping process, and it is expected to replace conventional doped-EMLs as emission layers. Except for its simple preparation process, it is more flexible in device design, more economical, and environmentally-friendly, and also can realize complete exciton utilization. (Xu et al., 2017; Luo et al., 2018; Zhang et al., 2020). The comprehensive comparisons for doped-EMLs and ultrathin-EMLs based OLEDs are in the [comparison for doped and ultrathin-EMLs based OLEDs](#) section. Hitherto, many works had been made to employ phosphorescent UEMls to develop high-performance OLEDs (Liu et al., 2016, 2019) and our group also did some attractive efforts (Miao et al., 2017b, 2018c, 2018d).

In this review, we summarized the research progress of UEMls-based OLEDs. Firstly, by comparing to conventional doped-EMLs-based OLEDs, it was demonstrated that phosphorescent UEMls are very advantageous for developing simplified but high performance OLEDs. Further, we carefully reviewed the research progress of UEMls-based OLEDs from the aspects of device design, fabrication process, operating mechanism, and device performance. In this section, we first discussed OLEDs with UEMls inserted into nonluminous materials, in which they can be divided into OLEDs with phosphorescent UEMl inserted into bulk and heterojunction interface; then we analyzed OLEDs with phosphorescent UEMls inserted directly into blue emitters including blue phosphorescent, conventional fluorescent, thermally activated delayed fluorescence (TADF), and exciplex emitters. In the end, we also provide a conclusion and prospected the future development of UEMls-based OLEDs. In this review, the full spellings for all specific materials are exhibited in [Table 1](#), and the device performance for the representative monochromatic and white OLEDs is summarized in [Table 2](#).

## COMPARISON FOR DOPED AND ULTRATHIN-EMLS BASED OLEDs

### Limitations of doped-EMLs in the development of OLEDs

The co-evaporation technology under a high vacuum is one of the most common methods used for fabricating doped-EMLs-based OLEDs, in which the doping concentration is realized by simultaneously controlling the deposition rates of the host and guest materials, as shown in [Figure 1](#).

**Table 1.** Abbreviation and full spelling for specific materials involved in this review

Abbreviation	Full name
TCTA	4,4',4''-Tris carbazol-9-yl)triphenylamine
CBP	4,4'-Bis(N-carbazolyl)-1,1'-biphenyl
mCP	1,3-Di-9-carbazolylbenzene
Ir(ppz) <sub>3</sub>	fac-tris(1-phenylpyrazolato-N,C2')-iridium (III)
Ir(picq) <sub>3</sub>	tris(1-phenylisoquinoline)iridium(III)
TPBi	1,3,5-Tris 1-phenyl-1H-benzimidazol-2-yl)benzene
TmPyPB	1,3,5-tri[(3-pyridyl)-phen-3-yl]benzene
Flrpic	Bis[2-(4,6-difluorophenyl)pyridinato-C2,N](picolinato)iridium(III)
Ir(ppy) <sub>2</sub> (acac)	bis 2-phenylpyridine)iridium acetylacetone)

(Continued on next page)

**Table 1. Continued**

Abbreviation	Full name
PO-01	Bis(4-phenyl-thieno[3,2-c]pyridinato-C2,N) (acetylacetone)iridium(III)
B3PYMPM	4,6-Bis(3,5-di (pyridin-3-yl)phenyl)-2-methylpyrimidine
(fbi)2Ir (acac)	bis 2-(9,9-diethyl-9H-fluoren-2-yl)-1-phenyl-1H-benzimidazole-N,C-3) iridium (acetylacetone)
(MDQ)2Ir(acac)	bis(2-methyldibenzo[f,h]-quinoxaline) (acetylacetone)iridium(III)
Ir (tfmppy)2 ttip	(tfmppy = 4-trifluoromethyl-phenylpridine, ttip = tetraphenylimido-diphosphinate)
Bphen	4,7-diphenyl-1, 10-Phenanthroline
Ir(ppy)3	Tris [2-(p-tolyl)pyridine-C2,N]iridium (III)
HAT-CN	2,3,6,7,10,11-Hexazatriphenylenehexacarbonitrile
TAPC	4,4'-cyclohexylidenebis[N,N-bis(p-tolyl)aniline]
Ir(bt)2(acac)	iridium(III)bis (2-phenylbenzothiozolato-N,C20)acetylacetone
TPXZPO	10, 10, 10-(4, 4, 4-Phosphoryltris(benzene-4, 1-diy))tris 10Hphenoaxazine)
B4PyPPM	4,6-Bis(3,5-di(pyridin-4-yl)phenyl)-2-phenylpyrimidine
26DczPPy	2,6-bis(3-(9H-carbazol-9-yl)phenyl)pyridine
BmPyPB	1,3-bis[3,5-di(pyridin-3-yl)phenyl]benzene
NPB	N,N'-Bis-(1-naphthalenyl)-N,N'-bis-phenyl-(1,1'-biphenyl)-4,4'-diamine
B3PYMPM	4,6-Bis(3,5-di (pyridin-3-yl)phenyl)-2-methylpyrimidine
PEDOT:PSS	Poly (3,4-ethylenedioxothiophene)-poly(styrenesulfonate)
Ir(tptpy)2(acac)	iridium(III)bis(4-(4-t-butylphenyl)thieno[3,2-c]pyridinato-N,C20)acetylacetone
mCBP	3,3'-Di(9H-carbazol-9-yl)biphenyl
PO-T2T	2,4,6-Tris[3-(diphenylphosphinyl)phenyl]-1,3,5-triazine
Bepp2	bis[2-(2-hydroxyphenyl)-pyridine]beryllium
Ir(piq)2(acac)	bis 1-phenyliso-quinoline)(acetylacetone)iridium(III)
Ir(ffpmq)2(acac)	(bis(2-(3-trifluoromethyl-4-fluorophenyl)-4-methylquinolyl) (acetyl-acetonate)iridium(III)
4P-NPD	N,N'-di-1-naphthalenyl-N,N'-diphenyl-[1,1':4',1":4",1'''-quaterphenyl]-4,4'''-diamine
RD01	iridium III)bis[2,-4-dimethyl-6-[5-(2-methylpropyl)-2-quinolinyl-N]phenyl-C]-[2,4-pentanedionato-O2,O4)
Ir tptpy)2 acac)	iridium III)bis (4-(4-t-butyl-phenyl)thieno[3,2-c]pyridinato-N,C20)acetylacetone

(Continued on next page)

**Table 1. Continued**

Abbreviation	Full name
DMAC-DPS	Bis[4-(9,9-dimethyl-9,10-dihydroacridine)phenyl]solfone
DPEPO	Bis [2-(diphenylphosphino)phenyl] iridium (III)bis(4-(4-t-butylphenyl)thieno[3,2-c]pyridinato-N,C20)acetylacetone
PO-01-TB	4,5-bis(carbazol-9-yl)-1,2-dicyanobenzene
2CzPN	bis(2-phenyl-4,5-dimethylpyridinato)[2-(biphenyl-3-yl)pyridinato]iridium-(III)
Ir (dmppy) <sub>2</sub> (dpp)	

In doped-EMLs-based OLEDs, a lower doping concentration makes the distance between host and dopant molecules exceed the radius of energy transfer, which leads to excitons on host diffuse firstly to another host molecule rather than dopants, inevitably causing energy loss. A higher doping concentration increases the  $\pi-\pi$  stacking interaction of emitter molecules, and makes more excitons aggregated in emitters, further inducing triplet-triplet annihilation (TTA). (Wang and Su, 2019; Li et al., 2016; Xie et al., 2020). All these seriously affect the EL performance of OLEDs with doped EMLs. Thus, a precise doping concentration for doped-EMLs is the prerequisite for realizing high device performance. However, it is very difficult to acquire an accurate concentration control, especially for single EML-based white OLEDs with two or more emitters simultaneously doped in a host, which greatly limits the development of doped-EMLs-based OLEDs to some extent (Zou et al., 2021; Wu and Ma, 2016). Moreover, for the doped-EMLs-based OLEDs, host materials are additionally introduced, and they are required to exhibit wide band gap, high triplet level ( $T_1$ ), high charge transport ability, matched highest occupied molecular orbital (HOMO), and lowest unoccupied molecular orbital (LUMO) levels with charge transporting materials (Yang et al., 2015; Jeon et al., 2021; Wei et al., 2020). However, it is difficult to design and synthesize suitable host materials for OLEDs. It is also hard to simultaneously realize effective emissions of different emitters by using the universal host, which greatly restricts the development of white OLEDs, where two or more host materials may be needed simultaneously to introduce into the device preparation (Liu et al., 2020; Park et al., 2018). Finally, the doped-EMLs-based OLEDs still suffer from high cost, which is not expected for commercialization. On the one hand, the high cost is caused by the low reproducibility for mass production of OLEDs by doping technology because of its stringent accuracy requirements for doping concentration in device fabrication process by multisource co-evaporation technology. On the other hand, the high cost results from the inefficient utilization of expensive phosphorescent materials. Assuming 10 vol% of expensive phosphorescent emitters doped in 10 nm-thick hosts are replaced with UEMls with a thickness of only 0.3 nm, which may be able to save at least 70% of materials cost (Wu et al., 2016). All above these become the limiting factors of the further development of doped-EMLs OLEDs.

### Working mechanism and advantages of UEMls-based OLEDs

To suppress above limiting factors of doped-EMLs, UEMls can be an ideal candidate for developing OLEDs because it avoids the use of doping technology but can realize the doping effect. It was demonstrated that the thickness of UEMls can be accurately controlled by monitoring the calibrated crystal quartz sensors connected with the quartz crystal vibration probe outside the vacuum chamber. In 2019, Reineke et al. carried out a comprehensive analysis about the optical properties of UEMls, and it was found that the red and green UEMls show a similar photoluminescence (PL) spectrum, PL quantum yield (PLQY), and emitter orientation with respect to the doped EMLs, implying that molecular aggregation, which would be detrimental for the performance, is negligible (Liu et al., 2019). In addition, some literature also confirmed that the introduction of UEMls has a negligible influence on the charge transport in devices. The reason is that interface energy barriers can be reduced because of the oppositional electric field by accumulating a significant number of electrons or holes. The number of accumulated electrons or holes in UEMls is small and the interface energy barrier is easy to overcome (Zhao et al., 2011; Liu et al., 2013a; Chen et al., 2016a). It can be proved by the similar current density-voltage (J-V) characteristics of devices with or without UEMls. In addition, the island structure of UEMls also makes it almost have no effect on the carrier distribution in the device, as mentioned in the introduction.

**Table 2.** The summary of device performance for representative OLEDs involved in this review

Ref	EML structure	Device performance			
		Maximum			
		CE (cd A <sup>-1</sup> )>	PE (lm W <sup>-1</sup> )	EQE (%)	Luminance (cd m <sup>-2</sup> )
Phosphorescent UEMLs inserted into single material					
Yang and Jabbour, 2013	FPt1/OXD-7 FPt1/OXD-7	–	–	18.1	8000
Zhao et al. (2013a)	Ir(piq) <sub>2</sub> (acac)/TCTA/Ir(fbi) <sub>2</sub> (acac)/TCTA/Ir(ppy) <sub>2</sub> (acac)/TCTA/Flrpic	21.1	23.0	10.8	40,600
Xue et al. (2015a)	PO-01/CBP/Flrpic	33.6	30.1	–	–
Wang et al. (2019b)	Ir(MDQ) <sub>2</sub> (acac)/mCP/PO-01/mCP/Ir(ppy) <sub>3</sub> /mCP/Flrpic	28.9	26.0	–	–
Phosphorescent UEML inserted into mixed materials					
Xue et al. (2015b)	PO-01/CBP:TPBi/TPBi:8%Flrpic	38.3	40.1	–	–
Yu et al. (2018)	Ir mphmq <sub>2</sub> (acac)/TCTA: Tm <sub>3</sub> PyPB/PO-01/TCTA: Tm <sub>3</sub> PyPB/Ir(ppy) <sub>2</sub> (acac)/TCTA: Tm <sub>3</sub> PyPB/Flrpic	44.9	42.5	16.1	–
Dai et al. (2019)	Flrpic/TCTA: TmPyPB/Ir(ppy) <sub>2</sub> (acac)/TCTA: TmPyPB/PO-01	55.2	57.6	16.0	–
Liu et al. (2019)	Ir(ppy) <sub>2</sub> (acac)mCP:B3PYMPM/Ir(ppy) <sub>2</sub> (acac) mCP:B3PYMPM/Ir(ppy) <sub>2</sub> (acac)	–	–	23.2	–
Phosphorescent UEML inserted in heterojunction interface without exciplex formation					
Zhao et al. (2013a)	TCTA/Flrpic/TmPyPB	37.0	43.0	17.1	22,000
	TCTA/(ppy) <sub>2</sub> Ir(acac)/TmPyPB	77.5	83.0	20.9	48,000
	TCTA/(fbi) <sub>2</sub> Ir(acac)/TmPyPB	47.5	51.0	17.3	38,000
	TCTA/(MDQ) <sub>2</sub> Ir(acac)/TmPyPB	29.8	32.0	19.2	30,000
Shi et al. (2014)	Ir(tfmppy) <sub>2</sub> (tpip)/TPBi/mCP/Ir(tfmppy) <sub>2</sub> tpip	126.3	–	–	–
Liao et al. (2019)	Ir(bt) <sub>2</sub> (acac)/TPXZPO/Flrpic	38.9	37.1	15.0	–
Zhang et al. (2018b)	TCTA/Beppz <sub>2</sub> /Ir(ppy) <sub>2</sub> (acac)	98.0	85.4	25.5	–
Phosphorescent UEML inserted into heterojunction interface with exciplex formation					
Qi et al. (2017b)	NPB/(btb) <sub>2</sub> Ir(acac)/B3PYMPM	53.3	53.1	19.5	17,400
Mu et al. (2019)	mCP/Flrpic/TmPyPB	–	50.8	17.7	–
Xu et al. (2017)	TAPC/Ir(ppy) <sub>2</sub> (acac)/TmPyPB	135.7	59.9	36.9	–
Xu et al. (2018)	TAPC/PO-01/TmPyPB	41.5	18.9	18.6	–
	TAPC/Flrpic/TmPyPB				
Li et al. (2018)	TCTA/Ir(ppy) <sub>2</sub> (acac)/B3PyMPM/Ir(ppy) <sub>2</sub> (acac) TCTA/Ir(ppy) <sub>2</sub> (acac)/B3PyMPM/Ir(ppy) <sub>2</sub> (acac) TCTA/Ir(ppy) <sub>2</sub> (acac)/B3PyMPM/Ir(ppy) <sub>2</sub> (acac) TCTA/Ir(ppy) <sub>2</sub> (acac)	84.5	92.8	26.9	–
Ying et al. (2020b)	Ir(tptpy)2acac/mCBP/Flrpic/PO-T2T/Ir(tptpy) <sub>2</sub> acac	70.0	91.5	21.3	–
Zhang et al. (2021b)	PO-01/mCBP:Flrpic	72.2	87.2	28.4	–
Phosphorescent UEML inserted in single-host forming blue phosphorescent EML					

(Continued on next page)

**Table 2. Continued**

Ref	EML structure	Device performance			
		Maximum			
		CE (cd A <sup>-1</sup> )>	PE (lm W <sup>-1</sup> )	EQE (%)	Luminance (cd m <sup>-2</sup> )
Zhu et al. (2014)	TCTA: Flrpic/Ir(bt) <sub>2</sub> (acac)/26DCzPPy: Flrpic	59.3	63.2	23.1	–
Wang et al. (2019b)	mCP: Flrpic/Ir(piq) <sub>2</sub> (acac)/mCP/PO-01/mCP/Ir(ppy) <sub>3</sub> /mCP: Flrpic	31.9	33.4	–	23,730
Wang et al. (2020)	mCP:Flrpic/Ir piq) <sub>2</sub> acac)/mCP/PO-01/NPB/TPBi/Ir(ppy) <sub>3</sub> /mCP:Flrpic	20.4	19.7	15.0	36,230
Phosphorescent UEMs inserted into mixed-host forming blue phosphorescent EML					
Chen et al. (2016b)	TCTA:TPBi:FlrPic/PO-01/TCTA:TPBi:FlrPic	39.8	40.8	–	–
Zhou et al. (2021)	mCP:TPBi:Flrpic/Ir ppy) <sub>3</sub> /Ir(piq) <sub>2</sub> (acac)/mCP:TPBi: Flrpic	14.66	15.35	–	9249
Wang et al. (2016)	PO-01/mCP: B3PYMPM: Flrpic	75.3	64.5	20.0	–
Phosphorescent UEMs inserted into conventional blue fluorescent EML					
Zhao et al. (2015)	Ir(ppy) <sub>2</sub> (acac)/TAPC/Bepp <sub>2</sub> /Ir(MDO) <sub>2</sub> (acac)	–	–	–	–
Miao et al. (2017b)	TCTA:Ir(ppb) <sub>3</sub> /TCTA/Bepp <sub>2</sub> /Ir(piq) <sub>2</sub> (acac)/Bepp <sub>2</sub> /TPBi/TPBi:Ir(fppmq) <sub>2</sub> (acac)	34.2	29.5	17.7	–
Miao et al. (2018c)	Bepp <sub>2</sub> /Ir piq) <sub>2</sub> (acac)/Bepp <sub>2</sub> /Ir(fppmq) <sub>2</sub> (acac) Bepp <sub>2</sub> /Ir(ppy) <sub>3</sub>	32.2	30.7	19.3	–
Miao et al. (2018d)	Ir piq) <sub>2</sub> (acac)/4P-NPD/4P-NPD:Bepp <sub>2</sub> /Ir(fppmq) <sub>2</sub> (acac)/4P-NPD:Bepp <sub>2</sub> /Bepp <sub>2</sub> /Ir(ppy) <sub>3</sub>	33.8	35.4	19.4	–
Chen et al. (2019)	RD071/4P-NPD/Ir(tptpy) <sub>2</sub> (acac)/4P-NPD/Bepp <sub>2</sub> /Ir(ppy) <sub>2</sub> (acac)/Bepp <sub>2</sub>	44.9	50.4	23.4	–
Phosphorescent UEMs inserted into blue TADF EML					
Qi et al. (2017a)	DPEPO: DMAC-DPS/(tbt) 2Ir(acac)/DPEPO: DMAC-DPS	45.2	45.8	15.7	10,150
Zhao et al., 2018a	Ir(MDO) <sub>2</sub> (acac)/DMAC-DPS/Ir(ppy) <sub>2</sub> acac)/DMAC-DPS/Ir(MDO) <sub>2</sub> (acac)	41.5	42.4	19.1	–
Dong et al. (2018)	mCP:2CzPN/PO-01-TB/mCP:2CzPN	65.9	79.2	22.3	–
Phosphorescent UEMs inserted into blue exciplex EML					
Luo et al. (2017)	Ir piq) <sub>3</sub> /TAPC/TmPyPB/Ir(dmppy) <sub>2</sub> (dpp)	26.9	28.2	15.1	–
Ying et al. (2018a)	mCBP:PO-T2T/Ir(tptpy) <sub>2</sub> (acac)/mCBP:PO-T2T	74.2	97.1	22.5	–
Ying et al. (2018b)	mCBP:PO-T2T:Flrpic/Ir(ppy) <sub>2</sub> (acac)/mCBP:PO-T2T:Flrpic	72.8	95.3	22.8	–

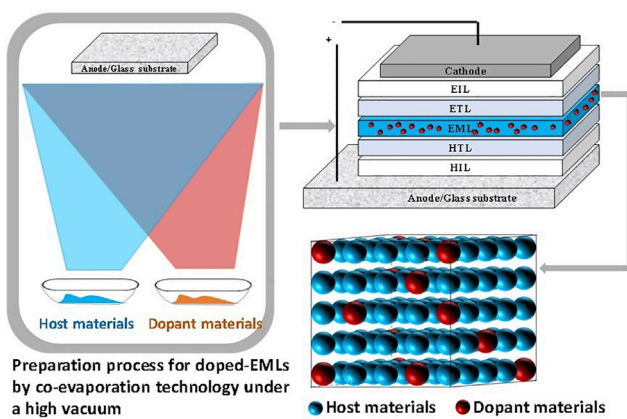


**Figure 1. Device fabrication and EMLs structure for host-guest system-based OLEDs**

The fabrication process and EMLs structure diagram for OLEDs with host-guest system using a doping technology under a high vacuum.

Because the carriers directly captured by UEMLS are almost negligible, most excitons used for molecular radiative transition are derived from the diffusion and energy transfer of the main recombination zone. Hence, the EL mechanism in UEMLS-based OLEDs is still mainly dominated by host-guest energy transfer. In a host-guest energy transfer system, charge carriers mainly transport and recombine on host molecules, so the J-V curves do not exhibit obvious sensitivity with the variation of doping concentration (Qi et al., 2017a). When UEMLS are inserted into the matrix, the matrix can be seen as the host, the variation of the thickness of UEMLS can be seen as the variation of doping concentration. If the J-V curves do not exhibit obvious sensitivity with the variation of the thickness of UEMLS, it can be inferred that carriers captured by UEMLS can be ignored. Besides, the transient EL curves without transient overshoots in the turn-off region also suggest that the emission mechanisms of phosphors are mainly stem from the energy transfer from hosts rather than the direct charge trapping on UEMLS molecules (Lee et al., 2013; Chen et al., 2020).

In order to increase the number of luminescent sites and avoid the mutual quenching of luminescent molecules simultaneously, several UEMLS need to be introduced into the same device, especially for white OLEDs. The thin organic layer (usually less than 5 nm) between UEMLS act as the carrier or exciton adjusting layer, was named as "spacer". For p-type and n-type spacer materials, they dominantly transport holes and electrons, respectively. However, when the spacers are thin enough, a portion of holes and electrons can transport across n-type and p-type spacers via the tunneling behavior, respectively (Liu et al., 2016; Lin et al., 2010). Besides, when the spacer is thin and the unoccupied sites exist, the excitons would penetrate spacer layers via unoccupied sites because of a long exciton diffusion distance, although the exciton energy of organic materials on both sides is higher than that of UEMLS (Miao et al., 2017b; Schwartz et al., 2009).

To sum up, the exciton diffusion and energy transfer may be abnormal when the organic layers are very thin. For phosphorescent UEMLS-based OLEDs, the light emission should be mainly originated from 1) the triplet excitons diffusion from main recombination zone to UEMLS because of the concentration gradient; 2) the excitons utilization formed in spacer; 3) the exciton formation in UEMLS by direct charge trapping, as shown in Figure 2.

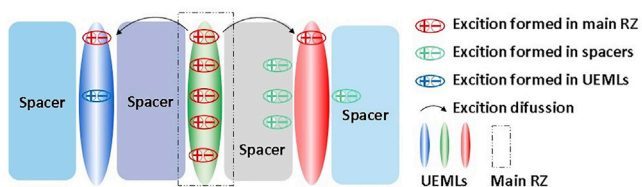


**Figure 2. Possible working mechanism for phosphorescent UEMLS-based OLEDs**

Three possible working mechanism for phosphorescent UEMLS-based OLEDs, where RZ is abbreviation of recombination zone. Herein, electron-hole pairs represent excitons formed in the form of charge transfer state or local excited state.

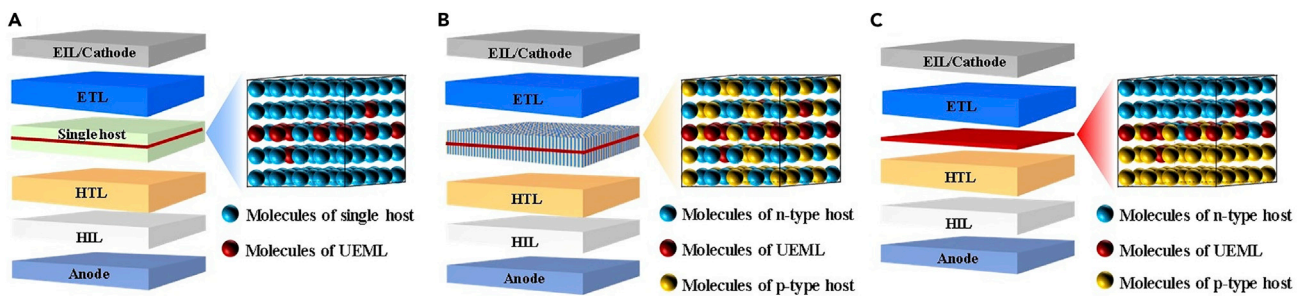


**Figure 3. Schematic device structure for OLEDs with UEMLs inserted into nonluminous materials**

Schematic device structure of OLEDs with phosphorescent UEMLs inserted into (A) single material, (B) mixed materials, and (C) heterojunction interface. Herein, HIL, HTL, ETL, and EIL are abbreviations of hole injection layer, hole transport layer, electron transport layer, and electron injection layer, respectively.

### OLEDS WITH UEMLS INSERTED INTO NONLUMINOUS MATERIALS

Phosphorescent UEMLs are sandwiched between nonluminous materials incipiently, and the spacer composed of nonluminous materials between UEMLs act as the carrier or exciton adjusting layer. The spacer has an important influence on device performance, so we classify and discuss OLEDs with UEMLs inserted into nonluminous materials according to spacer structure. In this section, UEMLs are inserted into the same materials (single material and mixed materials), which can be regarded as being doped in single host and mixed materials, respectively, as shown in Figures 3A and 3B. In addition, UEMLs are inserted into interfaces between different materials (interface without exciplex formation and interface with exciplex formation), which can be regarded as being doped in double hosts but without doping technique, as shown in Figure 3C.

#### OLEDs with phosphorescent UEMLs inserted into same material

##### Phosphorescent UEMLs inserted into single material

In general, holes and electrons mainly recombine in the organic layer between HTL (hole transporting layer) and ETL (electron transporting layer), which is structured by doping emitters into hosts in conventional host-guest system-based OLEDs. For UEMLs-based OLEDs, instead of doping emitter, phosphorescent UEML is directly inserted into common host materials such as TCTA (Zhao et al., 2013a; Tao et al., 2017; Zhang et al., 2017a), CBP (Liu et al., 2013b; Xue et al., 2015a, 2015b), and mCP (Tan et al., 2015; Xue et al., 2015c; Wang et al., 2019a, 2020; Yu et al., 2011; Yang et al., 2018) etc. Some work have been carried out for investigating the spatial distribution of excitons, and further revealed the effects of the thickness and position of UEMLs on the device performance in UEMLs-based OLEDs (Tan et al., 2015; Zhao et al., 2018b).

For example, in 2013, Jabbour et al. illuminated that the use of multiple phosphor/spacer layers as EML can help to minimize carrier recombination outside EML and resultantly reduce efficiency roll-off under high current density. (Yang and Jabbour, 2013). Besides, the EML consisting of multiple phosphor/spacer layers also provides the reference for designing white OLEDs which requires the introduction of more color emitters. Based on this, in the same year, Ma et al. developed several white OLEDs by incorporating complementary phosphorescent UEMLs into a single host of TCTA. TCTA, having high energy gap and triplet energy (3.40 and 2.86 eV), was used as interlayer to effectively suppress the energy transfer between phosphorescent UEMLs for realizing balanced white emission, achieving a high color rendering index (CRI) of 87 for four color white OLED at 1000 cd m<sup>-2</sup> (Zhao et al., 2013a).

CBP is a frequently used host for phosphors, and is also widely used as a spacer in UEMLs-based OLEDs. For example, in 2015, Xue et al. revealed the effect of thickness for CBP spacer on EL spectra in detail (Xue et al., 2015a, 2015b). They find when the thickness of CBP spacer is 3 or 4 nm, the light emitting unit could be regarded as “a single emission layer” with multiple doped dyes and no differential color aging, contributing to the excellent spectra stability. But when the thickness of CBP spacer is thicker, Dexter energy transfer from blue UEML to complementary yellow UEML becomes less efficient or is completely prevented. Thus, such devices could be considered as conventional white OLEDs with “multiple emission layers”.

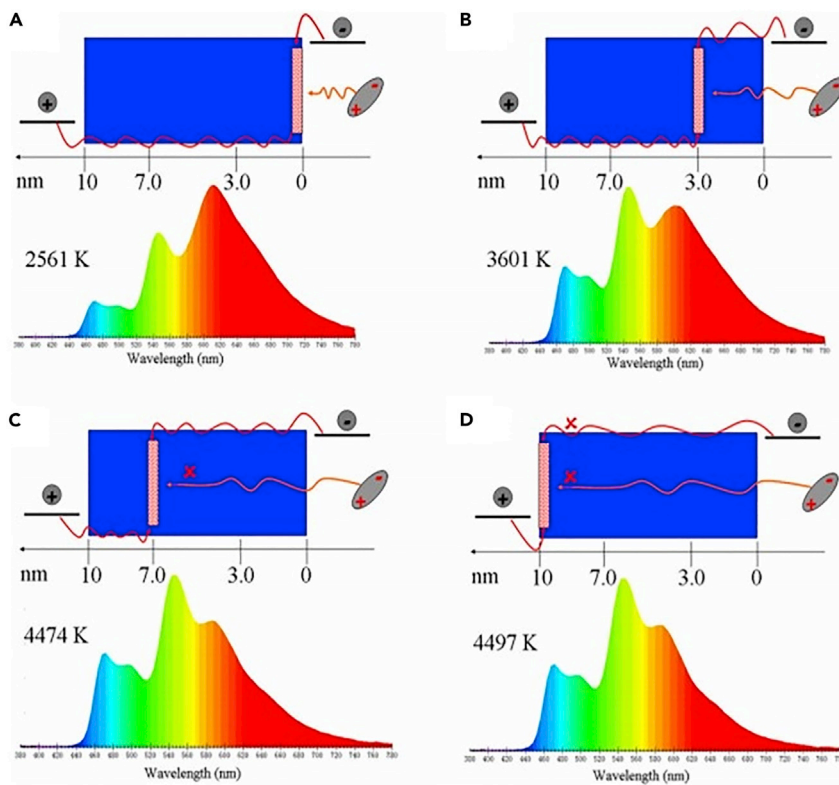


**Figure 4. Dynamic diagrams of charge carriers and excitons and corresponding EL spectra**

(A–D) Schematic diagram of dynamic of charge carriers and excitons and the corresponding EL spectra at 100 mA cm<sup>-2</sup> for devices with deep-red phosphorescent UEML of Ir(pic)<sub>3</sub> inserted into different positions of electron blocking layer Ir(ppz)<sub>3</sub>. Reproduced with permission (Xue et al., 2014), Copyright, AIP Publishing.

As a consequence, the relevant device exhibited a dramatic spectral change with thicker spacer. This is mainly because of the shift of carrier recombination zones in different color emission layers which is often observed in conventional multiple EMLs-based OLEDs.

Actually, a similar work is also carried out by employing mCP and Ir(ppz)<sub>3</sub> as spacers (Tan et al., 2015; Xue et al., 2015c; Yu et al., 2011). For example, Xue et al. inserted a deep-red phosphorescent UEML of Ir(pic)<sub>3</sub> into different positions of electron blocking layer Ir(ppz)<sub>3</sub>, and the objective is to distinguish the contribution of the emission from the triplet exciton energy transfer/diffusion from adjacent blue phosphorescent emitter and the trap-assisted recombination from the narrow bandgap emitter itself, as shown in Figure 4. It was demonstrated when the thickness of the spacer layer (Ir(ppz)<sub>3</sub>) increased to 7 nm, there was nearly no energy transfer detectable from blue phosphorescent emitter and red UEML. This indicates that a critical thickness value of 7 nm is extremely important for manipulating the energy transfer between different emitters on either side of the spacer layer, and further realizes high device performance (Xue et al., 2014).

#### Phosphorescent UEML inserted into mixed materials

It is difficult for a single material spacer to realize the balanced hole and electron transport, inducing an unbalanced exciton distribution in the EML zone. By comparison, the mixed materials spacer, formed by doped a hole transport material into an electron transport material, has many advantages (Lee et al., 2014a; Miao et al., 2019; Miao et al., 2018e). On the one hand, the mixed spacer is more favorable for designing device structure and reducing the energy barrier at interface for charge transport because electron and hole transport materials forming mixed spacer have more alternative energy levels, ensuring a good match with adjacent functional materials. On the other hand, the mixed spacer can achieve an approximately equal electron and hole mobility by precisely optimizing the doping ratio of hole transport material to electron transport material, which can effectively balance charge carrier transport and extend

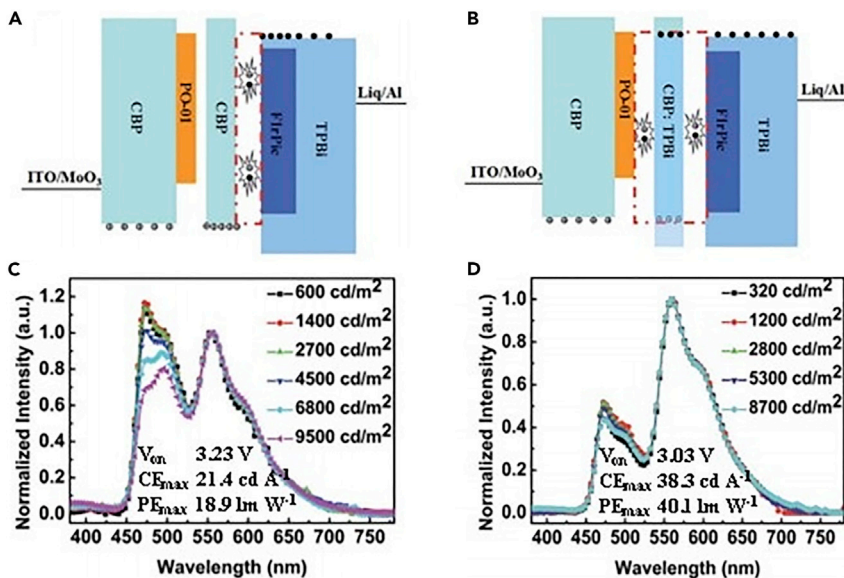


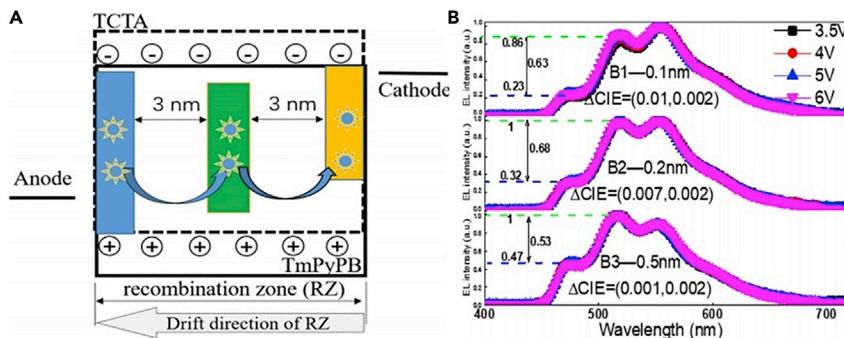
**Figure 5. Operational mechanism and EL spectra for two types of white devices**

Operational mechanism of white device based on uniform spacer (A) and based on mixed spacer (B). Normalized EL spectra and device performance of white device based on uniform spacer (C) and based on mixed spacer (D). Reproduced with permission (Xue et al., 2015b), Copyright, RSC Publishing.

exciton recombination zone. Thus, the mixed spacer is more popular for developing high device performance, and many endeavors have also been made by researchers in this connection.

In 2015, Xue et al. employed CBP:TPBi as the mixed spacer to construct complementary white OLEDs, and compare the operational mechanism with a CBP spacer-based device, shown in Figures 5A and 5B. It was demonstrated that the mixed spacer-based device showed a lower turn-on voltage than the uniform spacer-based device. In addition, the white device with the mixed ratio of 2:1 for CBP to TPBi achieves the high power efficiency which is 2.1 times as high as that of the device with a pure CBP spacer, and also exhibits excellent color stability, as shown in Figures 5C and 5D (Xue et al., 2015b). The similar effect has also been confirmed by Yu et al. They find when the mixed ratio for hole transporting TCTA to electron transporting TmPyPB is 3.5, the current density for corresponding hole-only and electron-only devices gets close to equilibrium, indicating the constructed mixed spacer realizes more balanced bipolar transport performance with respect to the synthetic bipolar host materials. Consequently, the fabricated three-colors and four-colors white OLEDs realize high current efficiency (CE) reaching 47.8 cd A⁻¹ and 44.9 cd A⁻¹, respectively. In addition, the Commission International de l' Eclairage (CIE) coordinates also shows a very slight variation of ( $\pm 0.02, \pm 0.02$ ) from 5793 cd m⁻² to 11,370 cd m⁻² for three-colors white OLED and ( $\pm 0.02, \pm 0.02$ ) from 3038 cd m⁻² to 13,720 cd m⁻² for four-colors white OLED, respectively (Yu et al., 2018).

However, hole and electron transport materials forming mixed spacer usually have different response on charge transport with increasing voltage, makes that the shift of carrier recombination zone with increasing voltage still exist in mixed spacer-based devices (Xue et al., 2015b; Yang et al., 2018). This will inevitably lead to the spectral changes and deterioration of spectra stability for white devices (Luo et al., 2018). But compared with conventional doped-EML-based white OLEDs, above adverse result can be easily suppressed by adjusting the thickness and sequence of phosphorescent UEML inserted in mixed spacer layer. (Dai and Cao, 2020; Dai et al., 2019). For example, Cao et al. fabricated three-color white OLEDs by incorporating complementary phosphorescent UEMLs into TCTA:TmPyPB-based mixed spacer with the structure of ITO/MoO<sub>3</sub>:TCTA(2:3, 35 nm)/TCTA(18 nm)/IrPic(x nm)/TCTA:TmPyPB(1:1, 3 nm)/Ir(ppy)<sub>2</sub>(acac)(0.15 nm)/ TCTA:TmPyPB(1:1, 3 nm)/ PO-01 (0.05 nm)/ TmPyPB(40 nm)/ LiF(1 nm)/ Al(100 nm), where x = 0.1, 0.2, and 0.5, respectively. In these devices, it is demonstrated that the direction of energy transfer is from IrPic UEML on the anode side to Ir(ppy)<sub>2</sub>(acac) UEML and then to PO-01 UEML on the cathode side, which is just opposite to the direction of carrier recombination zone, shown in

**Figure 6. Operational mechanism and EL spectra for UEMLs-based three-color white OLEDs**

Operational mechanism (A) and normalized EL spectra (B) for three-color white OLEDs with complementary phosphorescent UEMLs incorporated into TCTA: TmPyPB-based mixed spacer. Reproduced with permission (Dai et al., 2019), Copyright, IOP Publishing.

**Figure 6A.** Increasing the thickness of Flrpic UEML on the anode side can increase the efficiency of energy transfer, which can offset the effect of the drift of recombination zone and then obtain stable spectra, as shown in **Figure 6B** (Dai et al., 2019).

When the mixed spacer can form exciplex emission, it is demonstrated that bimolecular Langevin recombination was obviously enhanced, which make that the light emission is mainly produced by energy transfer from exciplex spacer to UEMLs rather than by trap-assisted Shockley–Read–Hall recombination (Wang et al., 2019b, 2019c; Lee et al., 2014b). Such an exciplex-spacer system is beneficial to dilute the excitons density in UEMLs and subsequently reduces the efficiency roll-off. Besides, exciplex spacer also provides an improved long-range coupled Förster energy transfer which also contributes to the realization of high efficiency (Tang et al., 2018; Wu et al., 2017; Tian et al., 2018; Shih et al., 2018). For example, in 2019, Sebastian Reineke et al. employ the exciplex of mCP:B3PYMPM(1:1, 5 nm) as mixed spacer, and the fabricated green-UEMLs-based and red-UEMLs-based OLEDs achieve the maximum external quantum efficiency (EQE) of 23.2 and 15.6%, and still remains at high values of 22.5 and 15.0% at 1000 cd m<sup>-2</sup>, respectively, which confirmed the advantage of exciplex spacers in developing high efficiency and low roll-off OLEDs (Liu et al., 2019).

### OLEDs with phosphorescent UEMLs inserted into heterojunction interface

#### Inserted in heterojunction interface without exciplex formation

Hole-transport material has a shallower HOMO level, and electron-transport material has a deeper LUMO level. A distinct energy level confines a large number of holes and electrons at the heterojunction interface, in which is the main carrier recombination zone. Introducing UEMLs at the heterojunction interface has been experimentally proved to be an effective way for making full use of excitons. For example, in 2013, 0.1 nm-thick blue (Flrpic), green (ppy)<sub>2</sub>Ir(acac), orange [(fbi)<sub>2</sub>Ir(acac)], and red [(MDQ)<sub>2</sub>Ir(acac)] UEMLs were inserted in TCTA/TmPyPB interface, respectively (Zhao et al., 2013a). As a comparison, monochromatic OLEDs with doped EML were also fabricated, where the host is either TCTA or TmPyPB. It reveals that in Flrpic-based and (MDQ)<sub>2</sub>Ir(acac)-based doped devices, using TCTA as host, nearly 100% exciton utilization is realized, whereas with TmPyPB as host, the excitons cannot be effectively utilized. For the cases of (ppy)<sub>2</sub>Ir(acac) and (fbi)<sub>2</sub>Ir(acac), the devices with TmPyPB as host show the highest efficiency whereas with TCTA as host there exists certain exciton quenching. Surprisingly, all UEMLs-based OLEDs achieve high efficiency with the maximum EQE reaching 17.1%, 20.9%, 17.3%, and 19.2% for blue, green, orange, and red devices, respectively, not affected by the contact of TCTA and TmPyPB. Similar work was also reported by Wu et al. (2016), indicating that the carriers and excitons at the interface can be almost completely utilized by phosphorescent UEMLs. In addition, these results also demonstrated the universality of the UEML for most phosphorescent dyes in such device structure.

Owing to the universality of UEMLs as mentioned above, the UEMLs inserted in the interface of hole-transport and electron-transport materials is also used in inverted OLEDs (Liu et al., 2014; Shi et al., 2014). In 2014, a bilayer TPBi/mCP is selected as spacer between green Ir(tfmpy)<sub>2</sub>(tpip)-based UEMLs in top-

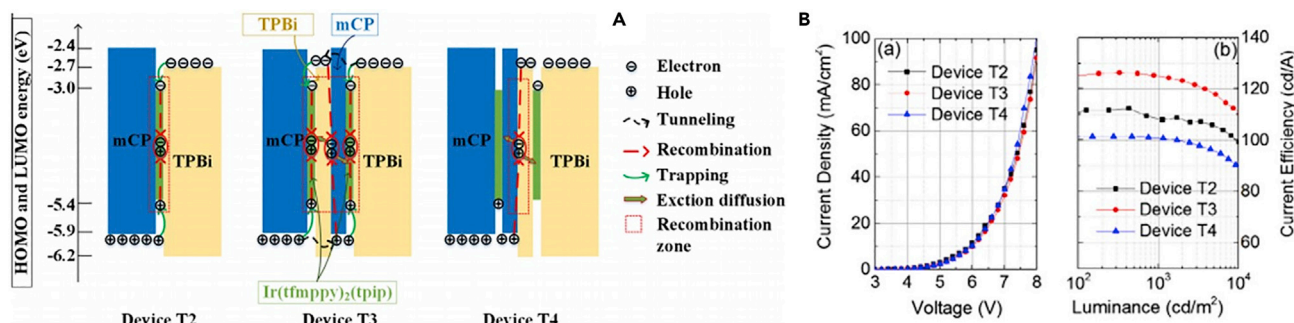


**Figure 7. Operational mechanism and EL performance for UEMLs-based OLEDs**

Operational mechanism (A) and J-V (on the left) and current efficiency-luminance (CE-L) (on the right) characteristics curves (B) of UEMLs-based inverted OLEDs. Reproduced with permission (Shi et al., 2014), Copyright, Elsevier.

emitting device by Shi et al. The device structure is Al/MoO<sub>3</sub>(3 nm)/mCP(50 nm)/ Ir(tfmppy)<sub>2</sub>(tpip)(0.5 nm)/ TPBi (2.5 nm)/ mCP (2.5 nm)/ Ir(tfmppy)<sub>2</sub>(tpip)(0.5 nm)/ TPBi(10 nm)/ Bphen(45 nm)/ Liq(1 nm)/ Al(1 nm)/ Ag(22 nm)/ mCP(80 nm). Herein, the thicker mCP and thin TPBi (2.5 nm) make the first UEML Ir(tfmppy)<sub>2</sub>(tpip) like "doping" in both mCP and TPBi host, so does the second UEML, as shown in Figure 7A. This structure is similar to dual "cohost" systems with thin thickness and is beneficial for carrier balance, which greatly improve the efficiency and avoid the doping process at the same time. The maximum CE reaches 126.3 cd A<sup>-1</sup> at 328 cd m<sup>-2</sup>, and still maintains to 125.0 cd A<sup>-1</sup> at 1000 cd m<sup>-2</sup>, shown in Figure 7B. The UEMLs can take full advantage of the cavity standing wave condition in inverted OLEDs with microcavity structure, hence the UEMLs-based OLEDs show much higher out-coupling efficiency than conventional doped-EMLs OLEDs. In addition, UEMLs inserted in interface is also used in tandem OLED, where a 0.25 nm-thick phosphorescent UEML sandwiched between TCTA/TmPyPB interface. The UEMLs along with non-doped charge generating unit (CGU) is a prospective strategy for simplified but high performance tandem OLEDs (Zhang et al., 2018a). However, it may not be suitable for structuring high color quality white OLEDs because such devices require the introduction of more complementary UEMLs, inducing more complicated device structure.

The thickness of phosphorescent UEMLs is also closely related to the device performance (Liu et al., 2013a; Xue et al., 2015a). In 2021, Kang et al. reported highly efficient green phosphorescent OLEDs by optimizing the thickness of Ir(ppy)<sub>3</sub>-based UEML. By carefully comparing two types of devices fabricated by UEML method and conventional doping method, they get the relationship between the device efficiency and average intermolecular distance of dopants according to the thickness in UEML method and the doping concentration in conventional doping method. As in Figures 8A and 8B, the device with 0.075 nm-thick UEML showed the highest EQE, in which was interpreted with average dopant intermolecular distance of 4 nm. In addition, the device with a doping concentration of 6 wt%, corresponding to the average dopant intermolecular distance of 3 nm, achieved the highest EQE. Herein, the average intermolecular distance of dopants was calculated by assuming that EML has a uniform molecular distribution for devices fabricated by adopting UEML method and conventional doping-EML method. On this basis, the thicknesses for hole-transport and electron-transport material were stepwise optimized to further improve device efficiency. Consequently, the maximum EQE of 23.8% is obtained, which is the highest EQE among Ir(ppy)<sub>3</sub> UEMLs-based OLEDs, shown in Figures 8C and 8D (Kang et al., 2021).

To develop white OLEDs, spacers are frequently introduced between different color UEMLs (Liu et al., 2016, 2017). Owing to different charge transport characteristics, the introduction of spacers can effectively manipulate the distribution of excitons on different color UEMLs for obtaining balanced white emission. In addition to the conventional host material (Zhang et al., 2017b), TADF molecules inherently possess donor and acceptor moieties, which potentially makes them ideal spacers with bipolar transport characteristics. The concept of TADF materials as spacers is proposed for the first time in 2019. The white OLEDs with structure of ITO/ HAT-CN(10 nm)/ TAPC(40 nm)/ mCP(15-x nm)/ Ir(bt)<sub>2</sub>(acac)(0.5 nm)/ TPXZPO(x = 1, 2, 3, 5, 10 nm)/ Flrpic (0.5 nm)/ B4PyPPM (40 nm)/ LiF(0.8 nm)/ Al(150 nm) was reported by Li et al. It was demonstrated that the carrier recombination zone was mainly located at the interlayer of blue TADF TPXZPO, which can ensure the efficient energy transfer and complete exciton harvesting for realizing highly efficient white light emission (Liao et al., 2019).

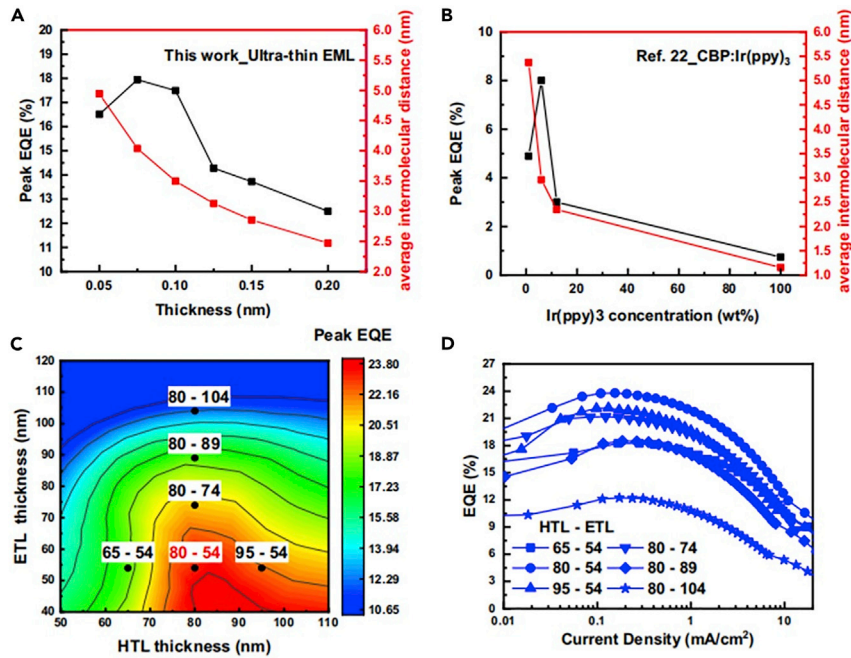


**Figure 8. Relation between EQE and average dopant intermolecular distance in OLEDs**

The relation between EQE and average dopant intermolecular distance according to the thickness of UEML (A) and doping concentration (B); EQE contour plot (C) and current density-EQE (J-EQE) characteristics curve (D) for all fabricated OLEDs with various values of HTL and ETL thickness. Reproduced with permission (Kang et al., 2021), Copyright, Springer Nature.

UEMLs incorporated into interface, where is main carrier recombination zone, easily causes excitons quenching. In order to reduce the quenching of excitons at the interface and improve efficiency stability, UEMLs are also incorporated away from the interface. For example, in 2017, Zhang et al. (2017a) proposed the high efficiency and low roll-off phosphorescent white OLEDs with the structure of ITO/ MoO<sub>3</sub>(10 nm)/ MoO<sub>3</sub>:TAPC(25wt%, 35 nm)/ TAPC(12 nm)/ TCTA(5 nm)/ Ir(MDQ)<sub>2</sub>(acac)(0.05 nm)/ TCTA(1 nm)/ FIrpic(0.4 nm)/ 26DCzPPy(2 nm)/ BmPyPB(2 nm)/ Ir(ppy)<sub>2</sub>(acac)(0.2 nm)/ BmPyPB(8 nm)/BmPyPB: Li<sub>2</sub>CO<sub>3</sub>(3 wt %, 25 nm)/Li<sub>2</sub>CO<sub>3</sub>(1 nm)/Al(150 nm). It can be seen that such a structure make red and green UEMLs far away from exciton formation region, as shown in Figure 9A. Therefore, the efficiency roll-off at a high luminance caused by exciton annihilation is significantly suppressed. The optimized white OLED achieves the high maximum EQE of 20.3%, and still remains 18.8% at 5000 cd m<sup>-2</sup>. In 2018, Zhang et al. (2018b) further inserted a green UEML into the proper position of ETL, away from the exciton recombination interface, to fabricate high efficiency and low roll-off green OLED. Compared to conventional UEMLs-based reference device, the exciton emission and exciton recombination in proposed device are completely separated, shown in Figure 9B. Therefore, the exciton quenching is greatly suppressed in this work. As a consequence, the target device exhibits the maximum CE, power efficiency (PE), and EQE of 98.0 cd A<sup>-1</sup>, 85.4 lm W<sup>-1</sup>, and 25.5%, and still reach 94.9 cd A<sup>-1</sup>, 55.5 lm W<sup>-1</sup>, and 25.1% at 5000 cd m<sup>-2</sup>, respectively.

#### Inserted into heterojunction interface with exciplex formation

In order to suppress the excitons quenching at heterojunction interface, phosphorescent UEMLs are also incorporated into such interface, in which there is exciplex formation. This is because the introduction of UEMLs would not impede the interaction between donor and acceptor at interface (Qi et al., 2017b; Zhang and Xie., 2019). As mentioned above, the UEMLs sandwiched between two materials can be considered as the emitter of UEMLs doped in two materials. Hence, Donor/UEMLs/Acceptor system can be regarded as exciplex as host of UEMLs emitter, which possess many advantages, such as reduced injection barrier, enhanced energy transfer, and reduced polaron quenching (Lee et al., 2013; Shin et al., 2014; Tian et al., 2020; Zhang et al., 2021).

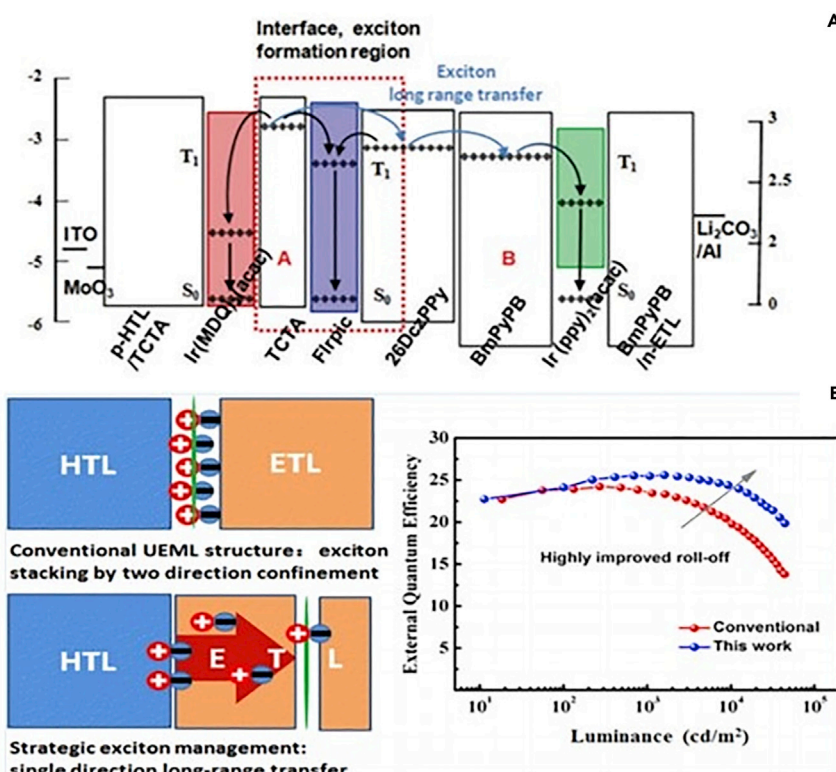


**Figure 9. Exciton distribution and transfer mechanism for UEMLs-based white OLEDs**

(A) Exciton transfer mechanism of white OLEDs with UEMLs incorporated away from main carrier recombination zone; Reproduced with permission (Zhang et al., 2017a). Copyright, Royal Society of Chemistry. (B) Comparison of exciton distribution and EQE-L characteristic curve for OLEDs with UEMLs incorporated into exciton formation interface and away from exciton formation interface. Reproduced with permission (Zhang et al., 2018b), Copyright, American Chemical Society.

Firstly, interface exciplex with TADF characteristic is adopted for highly efficient orange and blue phosphorescent OLEDs based on the above design concept of Donor/UEML/Acceptor. The orange phosphorescent OLED with the structure of ITO/MoO<sub>3</sub>(5 nm)/NPB(40 nm)/TCTA (10 nm)/(tbt)<sub>2</sub>Ir(acac)(0.3 nm)/B3PYMPM(10 nm)/Bphen (40 nm)/Mg:Ag 100 nm) exhibits the high CE, PE, and EQE of 53.3 cd A<sup>-1</sup>, 53.1 lm W<sup>-1</sup>, and 19.5%, respectively, and the light emission process is shown in Figure 10A. As the thickness of UEML increases to above 0.2 nm, orange molecules of (tbt)<sub>2</sub>Ir(acac) provide sufficient sites for exciton radiation; therefore, the emission peak originated from exciplex gradually disappears in EL spectra of corresponding devices, as shown in Figure 10B. The achievement for high efficiency is attributed to the efficient reverse intersystem crossing (RISC) process of exciplex and multiple host-guest energy transfer, as shown in Figure 10C (Qi et al., 2017b). The blue phosphorescent OLEDs with the structure of ITO/PE-DOT:PSS/TAPC(30 nm)/TCTA(4 nm)/mCP(5 nm)/Flpic(0.3 nm)/TmPyPB(45 nm)/LiF/Al also obtained the high device performance with the maximum PE and EQE reaching 50.82 lm W<sup>-1</sup> and 17.72%, respectively. In such a device, there are three radiative decaying processes involved, i.e., the prompt and delayed fluorescence processes of exciplex as well as the phosphorescence processes of UEML molecules, as shown in Figure 10D. In addition, the competition of those processes contributes to the realization of final high EL performance (Mu et al., 2019).

On the basis of the successful development in simplified but high efficiency devices based on the Donor/UEML/Acceptor structure, in 2017, Xu et al. designed tandem green OLED with Donor/UEML/Acceptor as light-emitting units. Specifically, they incorporated green Ir(ppy)<sub>2</sub>(acac)-UEML into interface of TAPC/TmPyPB exciplex with the detailed structure of ITO/HAT-CN(10 nm)/TAPC(55 nm)/Ir(ppy)<sub>2</sub>(acac)(0.8 nm)/TmPyPB(40 nm)/BPhen: LiNH<sub>2</sub>(10 nm, 50% by mole)/HAT-CN(10 nm)/TAPC(55 nm)/Ir(ppy)<sub>2</sub>(acac)(0.8 nm)/TmPyPB(40 nm)/Liq(2 nm)/Al(120 nm) (Xu et al., 2017). The resulting

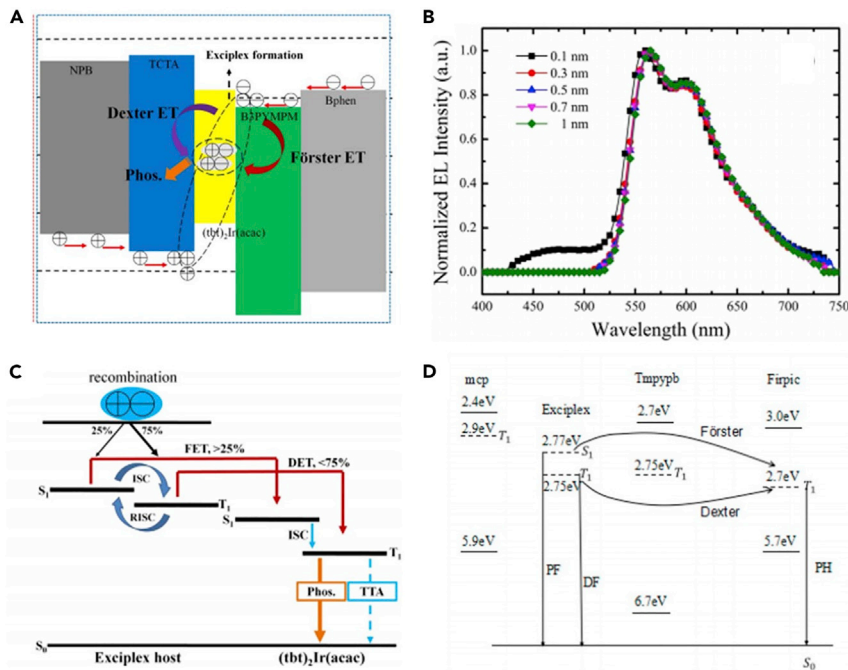


**Figure 10. Energy transfer, exciton decaying route, and EL spectra diagrams**

(A) Light emission process diagram for orange OLEDs with UEMLS inserted interface with exciplex formation; Reproduced with permission (Qi et al., 2017b), Copyright, Elsevier.

(B) Normalized EL spectra for above corresponding orange OLEDs at  $1000 \text{ cd m}^{-2}$ ; Reproduced with permission (Qi et al., 2017b), Copyright, Elsevier.

(C) Schematic EL mechanism diagram for above corresponding orange OLEDs with phosphorescent UEML thicknesses above 0.3 nm; Reproduced with permission (Qi et al., 2017b), Copyright, Elsevier.

(D) Schematic drawing of the possible energy transfer and exciton decaying route in the mCP/Firpic-UEML/TmPyPB-based blue phosphorescent OLEDs. Herein, FET, DET, and Phos are the abbreviations of Förster, Dexter energy transfer, and phosphorescence radiation, respectively. Reproduced with permission (Mu et al., 2019), Copyright, Elsevier.

tandem OLED exhibits the peak CE and EQE of  $135.74 \text{ cd A}^{-1}$  and 36.85%, respectively. In 2018, they further developed tandem white OLED by using Donor/UEML/Acceptor structure, where blue Firpic-UEMLs and yellow PO-01-UEMLs are implanted separately into interfaces of TAPC/TmPyPB exciplex using as two complementary light emitting units. The fabricated tandem white OLED obtains the maximum CE and EQE of  $41.5 \text{ cd A}^{-1}$  and 18.59% without light out-coupling technology. These works proved the feasibility of developing simple and efficient tandem OLEDs by simultaneously combining interfacial exciplex and phosphorescent UEMs strategy. However, to obtain high-color quality white emission still requires the introduction of three or more complementary light emitting units, showing complicated device structure and preparation process (Xu et al., 2018).

In 2018, Li et al. elected TCTA/B3PyMPM as interfacial exciplex, and incorporated  $\text{Ir}(\text{ppy})_2(\text{acac})$ -UEML into the interface of exciplex to realize extremely efficient green OLEDs having the maximum EQE and PE of 26% and  $93 \text{ lm W}^{-1}$ , respectively. Compared with non-exciplex-based devices, it is demonstrated that interfacial exciplexes as sensitizers effectively up-convert  $T_1$  excitons and this extra conversion can increase the population of  $S_1$  excitons, thus enhancing the energy transfer. This is the main reason for the proposed green OLED achieving extremely high efficiency. In order to improve efficiency roll-off, they further introduced several interfacial exciplex (TCTA/B3PyMPM) into the same device by vertical stacking method, creating multi-quantum-well (MQW) structure. It is revealed that the MQW structure can effectively disperse carriers and broaden the exciton recombination zone and simultaneously maximize the efficiency at high brightness, as illustrated from the distribution pattern in Figure 11. As the number of quantum-wells (QW) increases, the efficiency roll-off for the corresponding device is observably improved (Li et al., 2018). Besides, the MQW structure containing several vertical stacked interfacial exciplexes also offers the possibility of developing color quality white OLEDs by introducing phosphorescent UEMs into exciplex interfaces in the same single light-emitting unit device.

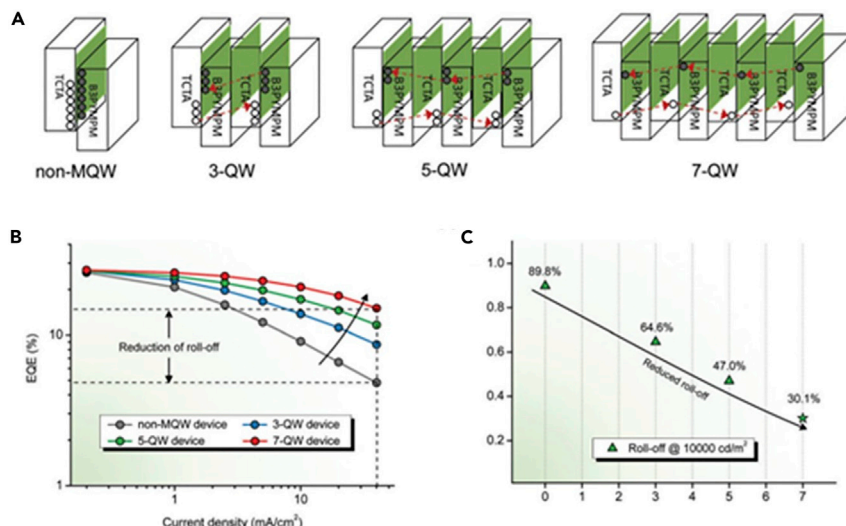


**Figure 11. Relation for MQM-based EML structure and efficiency roll-off characteristics**

(A) EML structure with non-MQW, 3-QW, 5-QW, and 7-QW, where the green color represents the UEML consisting of  $\text{Ir}(\text{ppy})_2\text{acac}$ ; (B) EQE-J characteristics curve; (C) Efficiency roll-off characteristics curve for the devices with different numbers of QW. Reproduced with permission (Li et al., 2018), Copyright, Royal Society of Chemistry.

When a phosphorescent UEML was inserted in heterojunction interface, a more efficient energy transfer occurs from interfacial exciplex to UEML dyes than the counterpart in non-exciplex-based devices (Wu et al., 2019; Wang et al., 2019d; Sheng et al., 2020). After understanding the luminescence mechanism of monochromatic OLEDs based on Donor/UEML/Acceptor structure, in 2020, Ma et al. reported a complementary color white OLED by simultaneously combining multi-UEMLs with interfacial exciplex, and the detailed device structure is ITO/ HAT-CN(15 nm)/ TAPC(55 nm)/ TCTA(10 nm)/  $\text{Ir}(\text{tpy})_2(\text{acac})(0.05 \text{ nm})$ / mCBP(2 nm)/ Flpic(0.3 nm)/ PO-T2T(2 nm)/  $\text{Ir}(\text{tpy})_2(\text{acac})(0.05 \text{ nm})/\text{PO-T2T}$  38 nm)/LiF(1 nm)/Al(150 nm). As shown in Figure 12A, singlet and triplet excitons are mainly generated in interfacial exciplex of mCBP/PO-T2T. The triplet excitons could undergo RISC to corresponding singlet excitons. The excitons transfer to blue UEML via Dexter and Förster energy transfer processes, resulting in blue emission, whereas the orange emission of two UEMLs originates from multi-Förster energy transfer channels from interfacial exciplex and Flpic. Benefiting from the multichannel energy transfer process, the targeted white OLED realizes the high forward-viewing CE, PE, and EQE of  $70 \text{ cd A}^{-1}$ ,  $91.5 \text{ lm W}^{-1}$ , and  $21.3\%$ , and still remain as high as  $53.6 \text{ cd A}^{-1}$ ,  $49.5 \text{ lm W}^{-1}$ , and  $16.7\%$  at  $1000 \text{ cd m}^{-2}$ , respectively, as shown in Figures 12B–12D (Ying et al., 2020b). Based on above multichannel energy transfer mechanism, in 2021, Zhang et al. also demonstrated two highly efficient white OLEDs, where the white devices are structured by strategically arranging orange phosphorescent UEMLs at two sides of blue phosphorescent doped layer. The interfacial exciplex can be formed between the host and electron transport material, ensuring multichannel energy transfer occurs for highly efficient exciton utilization. Consequently, the fabricated cold white OLEDs with CIE coordinates of (0.25, 0.39) exhibits a high maximum CE, PE, and EQE of  $72.17 \text{ cd A}^{-1}$ ,  $87.17 \text{ lm W}^{-1}$ , and  $28.37\%$ , and the corresponding indicators for warm white OLEDs with CIE coordinates of (0.33, 0.44) are  $67.70 \text{ cd A}^{-1}$ ,  $81.10 \text{ lm W}^{-1}$ , and  $23.80\%$  (Zhang et al., 2021b).

### OLEDS WITH PHOSPHORESCENT UEMLS INSERTED INTO BLUE EMITTERS

In the above review, phosphorescent UEMLs are inserted into nonluminous materials which can be regarded as being used as hosts or spacers. However, such device structure can consume extra energy owing to the nonluminous characteristic of hosts or spacers. Especially, to develop white OLEDs, it requires the introduction of more complementary UEMLs, complicating the device structure and preparation process. Thus, it is more potential to insert UEMLs of long wavelength phosphors into blue emitters for developing white OLEDs. Such white devices successfully avoid the use of extra host or spacer materials, effectively simplifying device structure. Herein, “blue emitters” involve several blue EMLs: Doping phosphor into the host forming blue phosphorescent EML, conventional blue fluorescent EML, doping, or single TADF materials forming blue EML and exciplex blue EML.

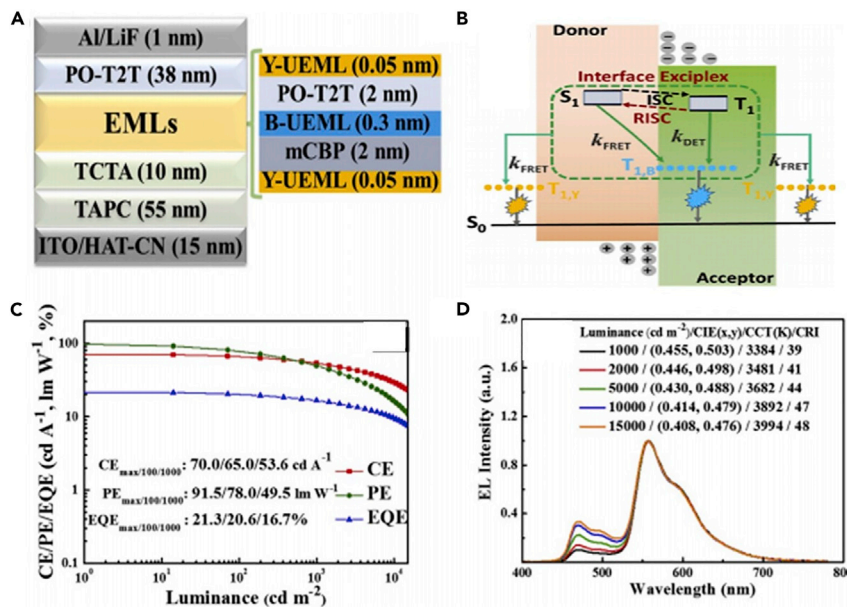


**Figure 12. Device structure, light emission mechanisms, and EL performance diagrams**

Device structure (A), light emission mechanisms (B), PE/CE/EQE-L characteristics curve (C), and normalized EL spectra at different luminance (D) for the proposed white OLEDs combining multi-UEMLs with interfacial exciplex. Reproduced with permission (Ying et al., 2020b), Copyright, Elsevier.

### Phosphorescent UEMls inserted into blue phosphorescent EMLs

#### Inserted into single-host forming blue phosphorescent EML

Few literature have reported that OLEDs using pure blue phosphor film as conventional EML achieved the satisfactory device performance because of severe exciton quenching induced by dense phosphorescent molecules. Thus, blue phosphors are usually doped into hosts (single material or mixed materials) to prepare doped film as blue phosphorescent EMLs, and the relevant blue phosphorescent OLEDs have achieved the extremely high EQE beyond the theoretical upper limit (Wang et al., 2016, 2020; Shin et al., 2014; Kang et al., 2016).

In earlier studies, researchers incorporated orange phosphorescent UEMl into the interfaces of single-host forming blue phosphorescent EML and electron-transport and hole-transport layers to report complementary white OLEDs, and the used structure as shown in Figures 13A and 13B (Wang et al., 2012; Zhao et al., 2013b). However, the low EL performance for reported white OLEDs make them not widely noticed. Until 2014, Ma et al. incorporated a yellow phosphorescent UEMl into interface of two blue phosphorescent EMLs to develop complementary white OLEDs with the EML structure of TCTA: 10 wt%Flrpic(5 nm)/Ir(b-t)<sub>2</sub>(acac)(x nm)/26DCzPPy: 20wt%Flrpic (5 nm), where x is 0.02, 0.04, 0.06, and 0.08 nm, respectively, as shown in Figure 13C. The optimized device (x = 0.04 nm) shows the high maximum CE, PE, and EQE of 59.3 cd A<sup>-1</sup>, 63.2 lm W<sup>-1</sup>, and 23.1%, which slightly reduce to 57.1 cd A<sup>-1</sup>, 53.4 lm W<sup>-1</sup>, and 22.2% at 1000 cd m<sup>-2</sup>, respectively, showing low efficiency roll-off, which is higher than most of the previously reported value in white OLEDs. However, the CRI for target device is less than 80 owing to a less spectral coverage in the visible band (Zhu et al., 2014).

One person wants to obtain the high CRI white light, it is a commonly used method to employ three or more emitters to structure white OLEDs. Hence, Kou et al. combine blue phosphorescent doped EML and green-phosphorescent, orange-phosphorescent, and red-phosphorescent UEMls to fabricate a series of white OLEDs with the EML structure of mCP: xwt%Flrpic(3 nm)/Ir(piq)<sub>2</sub>(acac) (0.15 nm)/mCP(3 nm)/PO-01(0.1 nm)/mCP(y nm)/Ir(ppy)<sub>3</sub> z nm)/mCP: 10 wt%Flrpic(3 nm), as shown in Figure 14A. The resulting device (x = 20, y = 1, z = 0.1) realize the ideal white light emission with CRI reaching 94 at 5 V, and the device (x = 20, y = 3, z = 0.05) exhibits more stable spectra with the CIE coordinates shift of only (0.0214, 0.0102) from 5 V to 8 V, as displayed in Figures 14B and 14C (Wang et al., 2019a). Further, replacing mCP spacer with multilayer

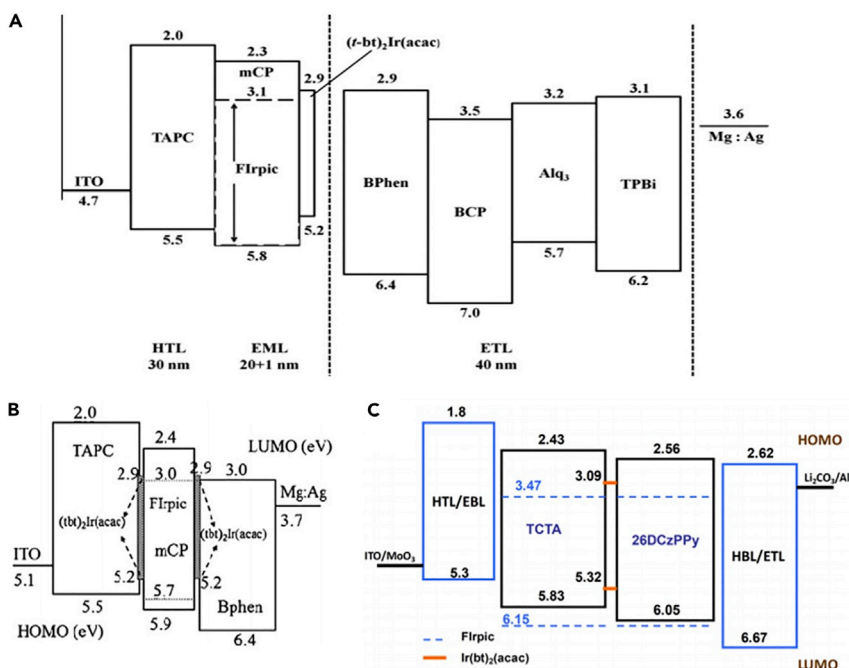


**Figure 13. Device structure and energy level diagrams**

The device structure and corresponding energy level diagrams for complementary white OLEDs with long-wave band phosphorescent UEML inserted in single-host forming blue phosphorescent EMLs zone. (A) Reproduced with permission (Wang et al., 2012), Copyright, Elsevier. (B) Reproduced with permission (Zhao et al., 2013b), Copyright, Elsevier. (C) Reproduced with permission (Zhu et al., 2014), Copyright, AIP Publishing.

mCP/NPB or NPB/TPBi, they fabricated another series of white OLEDs with the EML structure of mCP: 20wt %Flpic(3 nm)/ Ir(pic)<sub>2</sub>(acac)(0.15 nm)/ mCP(3 nm)/ PO-01(0.1 nm)/ mCP / mCP(3-x nm)/ NPB(x nm) (or NPB(3-y nm)/ TPBi(y nm))/ Ir(ppy)<sub>3</sub>(0.05 nm)/ mCP: 20 wt%Flpic(3 nm). They found that the thickness ratio of the planar heterojunction spacer (NPB/mCP or NPB/TPBi) between green and yellow UEMLs can change the direction of exciton energy transfer, as shown in Figure 14D. The fabricated white device with NPB(1.5 nm)/TPBi(1.5 nm) spacer displays a gradient enhanced EL spectra from blue light at short wavelengths to red light at long wavelengths, obtaining maximum CRI of 94 at 7.5V (Figure 14E). By reducing the doping concentration of Flpic in blue EML (close to ETL) to 3.3 wt%, the corresponding device achieves the maximum luminance of 36,230 cd m<sup>-2</sup>, and device show a slight CIE coordinates shift of (0.0440, 0.0029) from 5.5 V to 8.5 V. (Wang et al., 2020).

#### Inserted into mixed-host forming blue phosphorescent EML

Bipolar host materials can facilitate carrier injection, broaden carrier recombination one, and balance charge transport in EMLs, which are conducive to contributing to high EL performance. However, it is very difficult to design and synthesize single material with excellent bipolar transport characteristics and high triplet energy level, which make it suitable for use as a host of blue phosphorescent emitters. To solve this issue, researchers proposed mixed-hosts which were easily obtained by doping electron transport type hosts into hole transport type hosts. It was demonstrated that the mixed-host exhibited almost the same performance as the synthesized bipolar host by carefully controlling the doping ratio of the two host materials (Wei et al., 2017; Sheng et al., 2016; Jou et al., 2015).

In 2016, Chen et al. employed TCTA:TPBi as a mixed-host of blue FlPic, and inserted an orange UEML of PO-01 in the center of blue phosphorescent EML, to fabricate complementary white OLED with the structure of ITO/MoO<sub>3</sub>(2 nm)/TCTA(50 nm)/TCTA: TPBi: 10 wt%FlPic(2:1, 15 nm)/PO-01(0.1 nm)/TCTA: TPBi: 10 wt%FlPic(1:2, 15 nm)/TPBi(30 nm)/Liq(1 nm)/Al 100 nm). The mixed ratio of TCTA to TPBi in the mixed-host EML is assigned to 2:1 on the side near the pure TCTA layer and 1:2 on the side near the pure TPBi layer, respectively. Such clever design effectively reduced the interfacial energy barriers between EMLs and

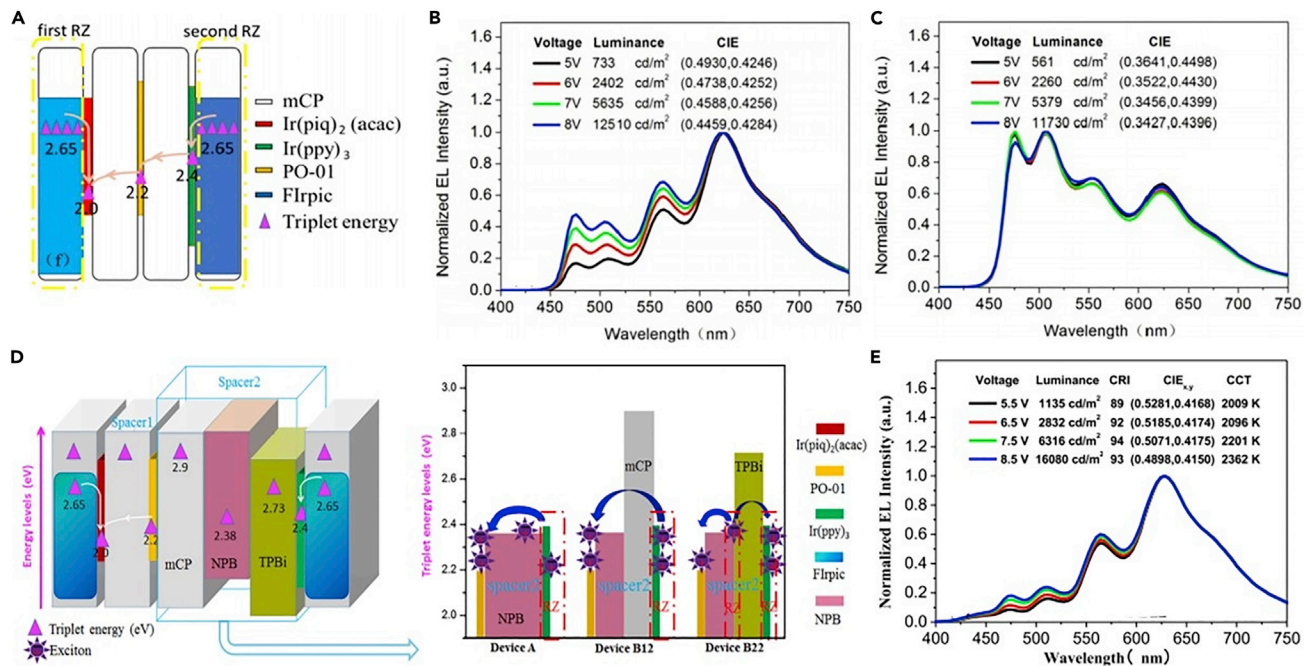


**Figure 14. Light-emitting mechanism and EL spectra diagrams**

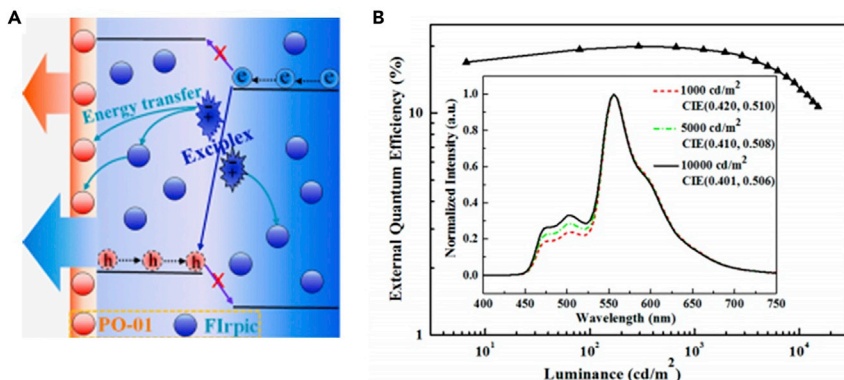
The light-emitting mechanism diagram (A) and normalized EL spectra (B and C) of the fabricated four color white OLEDs with mCP as spacer layer; Reproduced with permission (Wang et al., 2019a), Copyright, Elsevier. The light-emitting mechanism diagram (D) and normalized EL spectra (E) of the fabricated four color white OLEDs with multilayer mCP/NPB or NPB/TPBi as spacer layers. Reproduced with permission (Wang and Su, 2020), Copyright, Elsevier.

charge transport layers, and also ensured a wider carrier recombination zone throughout the whole EML. In return, the related white OLED realizes high device performance with peak efficiencies of  $40.8 \text{ lm W}^{-1}$  and  $39.8 \text{ cd A}^{-1}$ , and exhibits a low efficiency roll-off (Chen et al., 2016b). In 2021, Kou et al. adopted mCP: TPBi as mixed-host of blue Flrpic, and incorporated green-UEMLs and red-UEMLs into the middle of blue phosphorescent EML, to develop three color white OLEDs. A systematic study about the position and thickness of UEMs and the concentration of mCP in mixed-host EML was carried out, realizing the effective manipulation of carriers recombination zone and energy distribution. Consequently, a simple color-tunable all-phosphorescent white OLED emitting sunlight-style emission with a wider correlated color temperature (CCT) span (2391–6423 K) is realized (Zhou et al., 2021).

In addition, some mixed-hosts can form exciplex emission from intermolecular charge transfer of electron-transport and hole-transport type host materials. To insert complementary UEM into exciplex-based mixed-host layer is also applied to develop white OLEDs, and it is demonstrated that such device can realize more efficient utilization of excitons via exciplex energy transfer mechanism (Wang et al., 2016; Chen et al., 2017; Ying et al., 2019). For example, in 2016, an efficient exciplex of mCP: B3PYMPM was applied as the host of blue Flrpic by Ma et al., and they successfully fabricated white OLEDs by simply inserting an orange UEM within the blue emissive zone with the structure of ITO/MoO<sub>3</sub>(10 nm)/TAPC: 10 wt %MoO<sub>3</sub>(50 nm)/TAPC(20 nm)/PO-01 (0.06 nm)/mCP:B3PYMPM:Flrpic 1:1:0.4, 10 nm)/B3PYMPM(15 nm)/B3PYMPM: 3 wt%Li<sub>2</sub>CO<sub>3</sub>(40 nm)/Li<sub>2</sub>CO<sub>3</sub>(1 nm)/Al. (Wang et al., 2020). The target device achieves the maximum forward-viewing CE, PE, and EQE of 64.5 cd/A, 75.3 lm/W, and 20.0%, respectively, and remains 62.8 cd/A, 63.1 lm/W, and 19.5% at a luminance of 1000 cd/m<sup>2</sup>. The efficient utilization of excitons and the wide recombination zone are the key factors for the prominent achievement of high efficiency and low efficiency roll-off, as shown in Figure 15.

#### Phosphorescent UEMs inserted into conventional blue fluorescent EML

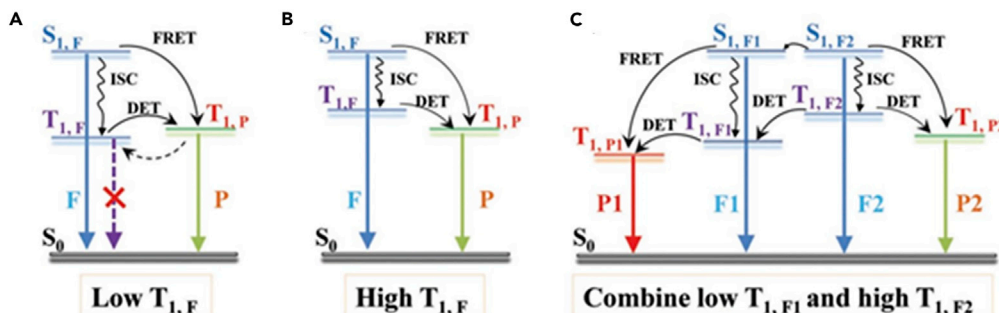
Considering blue phosphors easily suffer chemical degradation during device operation and there are still no ideal blue phosphorescent emitters in terms of lifetime and color stability, the development of all



**Figure 15. Light-emitting mechanism and EL performance diagrams**

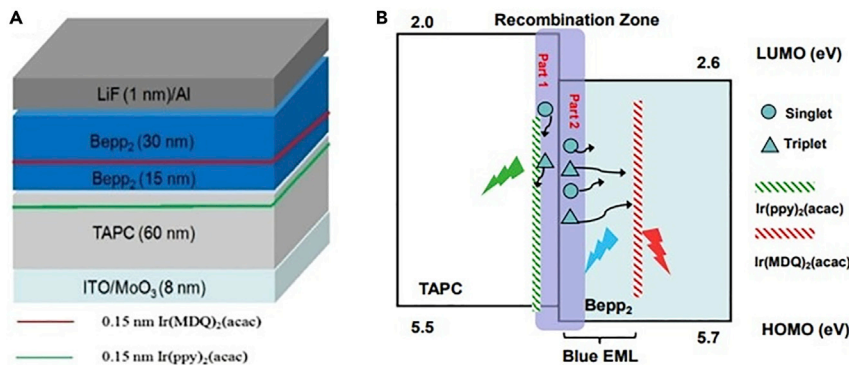
The light-emitting mechanism (A) and EQE-L characteristic curve (B) diagrams of complementary white OLEDs combining exciplex-based mixed-host and phosphorescent UEML, and the inset in (B) is the normalized EL spectra and CIE coordinates of corresponding white device at different luminance levels. Reproduced with permission (Wang et al., 2020), Copyright, American Chemical Society.

phosphorescent blue and white OLEDs is greatly restricted (Zhu et al., 2017; Yin et al., 2014). Instead, hybrid white OLEDs, structured by using blue fluorophores and complementary long wavelength phosphors, have drawn considerable attention because of their advantages of simultaneously combining the excellent stability of blue fluorophores and the high efficiency of long wavelength phosphors. (Zhao et al., 2018a; Dai and Cao, 2020; Sheng et al., 2019; Miao et al., 2017c; Yao et al., 2021). Thus, hybrid white OLEDs can theoretically realize 100% exciton utilization and exhibit high operational stability. According to the difference of  $T_1$  of selected blue fluorescent materials and complementary phosphors, the hybrid white OLEDs mainly involve two kinds of energy transfer processes (Chen et al., 2019). When the  $T_1$  for blue fluorophores is below that of complementary phosphors, the energy transfer of triplet excitons from phosphors to blue fluorophores can occur, as shown in Figure 16A. To stop such energy transfer that does not contribute to light emission, the spacers with relatively higher  $T_1$  than blue fluorophores are usually introduced between blue fluorescent layer and complementary phosphorescent layer, ensuring complete exciton utilization. Another is adopting a higher  $T_1$  of blue fluorophores, as shown in Figure 16B. In this case, the triplet excitons of blue fluorophor can be harvested by the phosphor for emission. Besides, there is no need to introduce a mandatory spacer between fluorescent and phosphorescent layers, giving a more flexible design for white OLEDs. In addition, if one person simultaneously employs two blue fluorophors, the energy transfer between both blue fluorophors is also involved, as shown in Figure 16C. This design is more conducive to develop high color quality white OLEDs containing multiple color emission.



**Figure 16. Schematic exciton energy transfer in hybrid white OLEDs**

(A) Blue fluorophore with a relatively lower  $T_1$  than that of complementary phosphors; (B) Blue fluorophor with a relatively higher  $T_1$  than that of complementary phosphors; (C) Two blue fluorophors are introduced and they have relatively higher  $T_1$  than those of corresponding phosphors adjacent themselves, respectively. Reproduced with permission (Chen et al., 2019), Copyright, John Wiley and Sons.

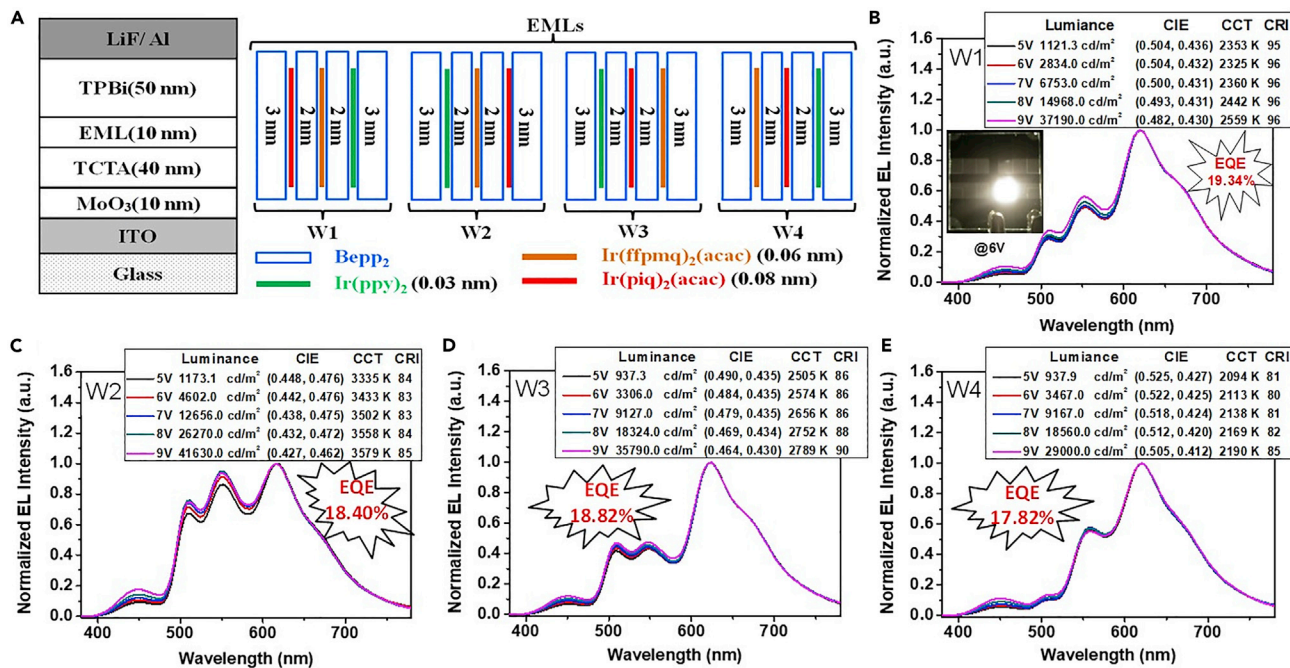
**Figure 17. Device structure and operational mechanism diagrams**

The device structure (A) and operational mechanism (B) diagrams for the proposed first three primary color doping-free hybrid white OLEDs. Reproduced with permission (Zhao et al., 2015), Copyright, Elsevier.

To design and construct hybrid white OLEDs, it is the prerequisite to select suitable blue fluorescent material. However, blue fluorescent materials with high efficiency and high  $T_1$  are fewer. Electron transporting Bepp<sub>2</sub> emits pure blue with emission peak at about 440 nm, and possesses higher  $T_1$  of 2.6 eV than most phosphors. In 2015, Ma et al. selected Bepp<sub>2</sub> as blue fluorophore to report the first three primary color doping-free hybrid white OLEDs by embedding green and red UEMLs on either side of hole (TAPC)/electron (Bepp<sub>2</sub>) transport layers (Zhao et al., 2015), as shown in Figure 17A, in which a green UEML is arranged on one side of the TAPC layer in the carrier recombination zone, but a red UEML is inserted into one side of the Bepp<sub>2</sub> layer away from the main carrier recombination zone. Such an elaborate design guaranteed that green phosphorescent UEML can directly harvest generated excitons within hole transporting TAPC layer, whereas singlet and triplet excitons generated in electron transporting Bepp<sub>2</sub> layer are spatially separated by their different diffusion lengths and used as blue emission of Bepp<sub>2</sub> and red emission of phosphorescent EML, respectively, as displayed in Figure 17B. Thus, the target device emits ideal white light with CIE coordinates of (0.44, 0.45) and high CRI of 82 at 1000 cd m<sup>-2</sup>, and realizes enhanced utilization of excitons with maximum CE reaching 23.2 cd A<sup>-1</sup>.

In 2017, using Bepp<sub>2</sub> as blue fluorescent material, our group reported a tetrachromatic hybrid white OLEDs with Bepp<sub>2</sub>-based blue fluorescent EML sandwiched between a pair of phosphors-doped HTL and ETL. By controlling the location of the green phosphor doped in HTL and yellow phosphor doped in ETL at ~1 nm away from the HTL/EML and EML/ETL interfaces, and incorporating a 0.1 nm-thick red phosphorescent UEML in the center of the Bepp<sub>2</sub> EML, The resulting device realizes the precise manipulation and effective exploitation of singlet and triplet excitons, contributing to ideal warm white emission, showing stable EL spectra with a maximum CRI of 94, a low CCT of 2440-2468 K over a wide voltage range of 5-9 V (Miao et al., 2017b). In our further research, the higher performance tetrachromatic hybrid white OLED, without using doping technology, is demonstrated with the detailed structure of ITO/ MoO<sub>3</sub>(3 nm)/ TCTA(40 nm)/ Bepp<sub>2</sub>(3 nm)/ Ir(piq)<sub>2</sub>(acac)(0.08 nm)/ Bepp<sub>2</sub>(2 nm)/ Ir(ppmq)<sub>2</sub>(acac)(0.06 nm)/ Bepp<sub>2</sub>(2 nm)/ Ir(ppy)<sub>3</sub>(0.03 nm)/ Bepp<sub>2</sub>(3 nm)/ TPBi(50 nm)/ LiF(1 nm)/ Al (200 nm), shown in Figure 18A. This device (EML1) exhibits a candle light-type warm white light emission with an ultrahigh CRI of 96 and a high EQE of 19.34%, and shows extremely stable EL spectra at a wide voltage range of 5 V-9 V, as displayed in Figure 18B. To the best of our knowledge, this is the first white OLED with good tradeoff among device efficiency, CRI, and color stability. What's more, the EL spectra of the hybrid white OLEDs can be easily adjusted by only changing the incorporating sequence of complementary phosphorescent UEMLs without device efficiency loss, as shown in Figures 18A and 18C-18E (Miao et al., 2018c).

Considering a relatively low PLQY of about 0.80 for Bepp<sub>2</sub>, several works incorporated a more efficient blue fluorophore of 4P-NPD with a PLQY as high as 0.92 to design blue fluorescent layer of hybrid white OLEDs (Miao et al., 2018e; Chen et al., 2018). 4P-NPD and Bepp<sub>2</sub> transport hole and electron carrier, respectively, and have nearly the same charge mobility of  $6.6 \times 10^{-4}$  cm<sup>2</sup> V<sup>-1</sup> second<sup>-1</sup> for 4P-NPD and  $10^{-4}$  cm<sup>2</sup> V<sup>-1</sup> second<sup>-1</sup> for Bepp<sub>2</sub>. This inspired us to design a very simple sandwich blue light device with the structure of ITO/MoO<sub>3</sub>/4P-NPD/4P-NPD:Bepp<sub>2</sub>/Bepp<sub>2</sub>/LiF/Al. The almost identical charge transport capacity for 4P-NPD and Bepp<sub>2</sub> make carrier recombination zone mainly located at middle mixed 4P-NPD:Bepp<sub>2</sub> layer and

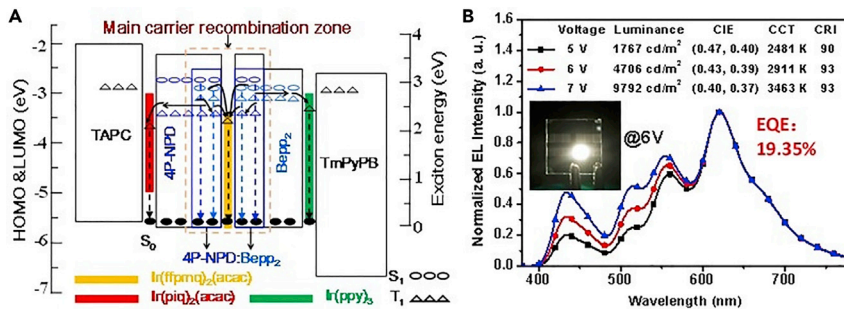


**Figure 18. Device structure and EL spectra diagrams**

The device structure diagram (A) and normalized EL spectra at different voltage (B-E) for corresponding hybrid white OLEDs with the different incorporating sequence for complementary green, yellow, and red phosphorescent UEMls in Bepp<sub>2</sub>-based blue fluorescent layer. Reproduced with permission (Miao et al., 2018c).

have a balanced distribution, which contributes to an extremely high EQE of 5.92% exceeding the theoretical upper limit (5%). In addition, the wider blue peak simultaneously combining the emissions of 4P-NPD and Bepp<sub>2</sub> is beneficial for developing white OLEDs. Thus, a tetrachromatic hybrid white OLED is proposed with the structure of ITO/MoO<sub>3</sub>(3 nm)/ TAPC(40 nm)/ Ir(piq)<sub>2</sub>(acac)(0.1 nm)/ 4P-NPD(3 nm)/ 4P-NPD : Bepp<sub>2</sub>(1:1, 3 nm)/ Ir(fppmq)<sub>2</sub>(acac)(0.03 nm)/ 4P-NPD : Bepp<sub>2</sub>(1:1, 3 nm)/Bepp<sub>2</sub>(3 nm)/Ir(ppy)<sub>3</sub>(0.2 nm)/ TmPyPB(50 nm)/LiF(1 nm)/Al 100 nm). The bidirectional exciton energy transfer from middle blue fluorescent layer of 4P-NPD:Bepp<sub>2</sub> to red and green UEMls on both sides guarantees a wide emission spectra, and the central yellow UEMl further consume a portion of generated singlet and triplet excitons in mixed 4P-NPD:Bepp<sub>2</sub> layer, leading to the broader emission spectra and more efficient utilization of excitons because of the reduced excitons loss caused by the long-length diffusion of triplet excitons (Miao et al., 2018d). The proposed tetrachromatic white OLED simultaneously achieved a high maximum EQE of 19.35% and a high CRI of 93%. The working mechanism and corresponding EL spectra at different voltage are presented in Figure 19.

Based on the bidirectional exciton energy transfer above mentioned, in 2019, Ma et al. also fabricated four color hybrid white OLEDs by implanting red and yellow phosphorescent UEMls in blue emitting 4P-NPD HTL with two UEMls separated by 4P-NPD, and inserting a green UEMl in blue emitting Bepp<sub>2</sub> ETL. The detailed structure is ITO/HAT-CN(15 nm)/ TAPC(65 nm)/ 4P-NPD(3 nm)/ RD071(0.32 nm)/ 4P-NPD(3 nm)/ Ir(tptpy)<sub>2</sub>(acac)(0.24 nm)/ 4P-NPD(5 nm)/ Bepp<sub>2</sub>(3 nm)/ Ir(ppy)<sub>2</sub>(acac)(0.24 nm)/Bepp<sub>2</sub>(47 nm)/Liq(1.25 nm)/ Al, as displayed in Figure 20A (Chen et al., 2019). Carrier recombination zone is mainly concentrated at the interface between 4P-NPD and Bepp<sub>2</sub>. The reasonable arrangement with UEMls more than 3 nm away from the interface between 4P-NPD/Bepp<sub>2</sub> ensure effective blue light emission intensity. Meanwhile, the precise thickness control of spacer layer between UEMls make the efficient stepwise energy transfer occurs from blue light to green and yellow light, and then to red light, guaranteeing the emission intensity of green, yellow, and red light, and the luminous mechanism was shown in Figure 20C. Thus, the resulting OLED emits a balanced warm white light with maximum CRI up to 95, and the device maintains the stable EL spectra at a wide luminance range from 1 to 10,000 cd m<sup>-2</sup> (Figure 20B). Further, the above white OLED also gets the high maximum CE, PE, and EQE reaching 44.9 cd A<sup>-1</sup>, 50.4 lm W<sup>-1</sup>, and 23.4%, and they still

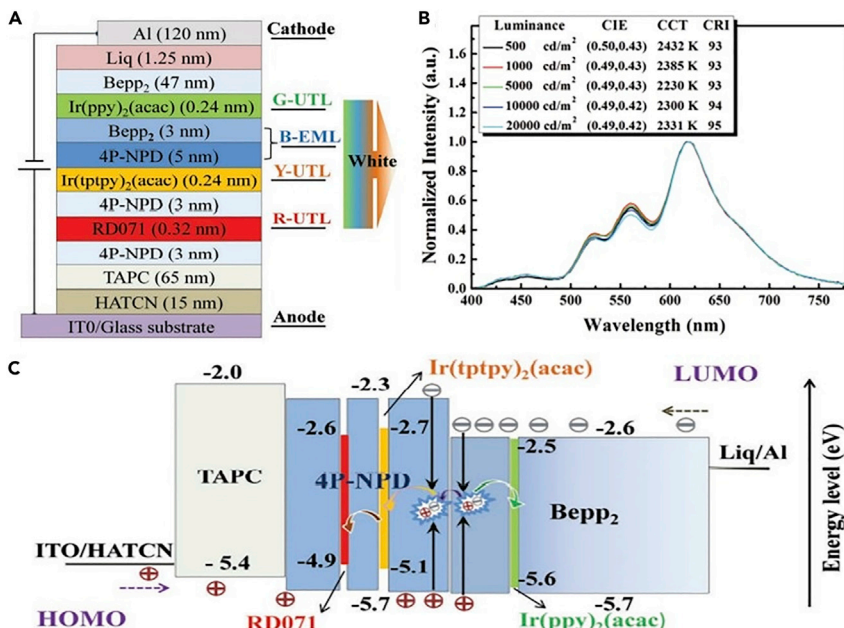
**Figure 19.** Light-emitting mechanism and EL spectra diagrams

The light-emitting mechanism (A) and normalized EL spectra at different voltage (B) diagrams for the proposed tetrachromatic hybrid white OLEDs with green, yellow, and red phosphorescent UEMls incorporated into a sandwich blue fluorescent emission zone. Reproduced with permission (Miao et al., 2018d), Copyright, Royal Society of Chemistry.

remain as high as 39.5 cd A<sup>-1</sup>, 31.2 lm W<sup>-1</sup>, and 20.3%, at 1000 cd m<sup>-2</sup>. The very bright EL performance further proves the potential and advantages of combining conventional fluorescent layer with phosphorescent UEMls structure to develop high-performance white OLEDs.

### Phosphorescent UEMls inserted into blue TADF EML

TADF emitters are considered as promising alternatives to replace the conventional blue fluorescent emitters in developing hybrid white OLEDs (Zhang et al., 2018c, 2021c; Ban et al., 2019; Li et al., 2021; Chen et al., 2021). The reasons are follows as: Firstly, blue TADF emitters possess high  $T_1$  and high efficiency compared with the conventional blue fluorescent emitters because of their sufficiently small energy gap between the singlet and triplet states and the potential of realizing exciton utilization of 100%; Second, blue TADF emitters usually exhibit the good bipolar transport characteristics because of the natural existence of donor and acceptor segments that could transport the holes and electrons, respectively, which can contribute to a broadened carrier recombination zone; Third, recent research works proved that many blue

**Figure 20.** Schematic structure, exciton transfer paths, and EL spectra diagrams

Schematic structure (A), normalized EL spectra at different luminance (B), and energy level of the used emitters and possible exciton transfer paths diagrams (C) for the designed four color hybrid white OLEDs by Ma et al. Reproduced with permission (Chen et al., 2019), Copyright, John Wiley and Sons.

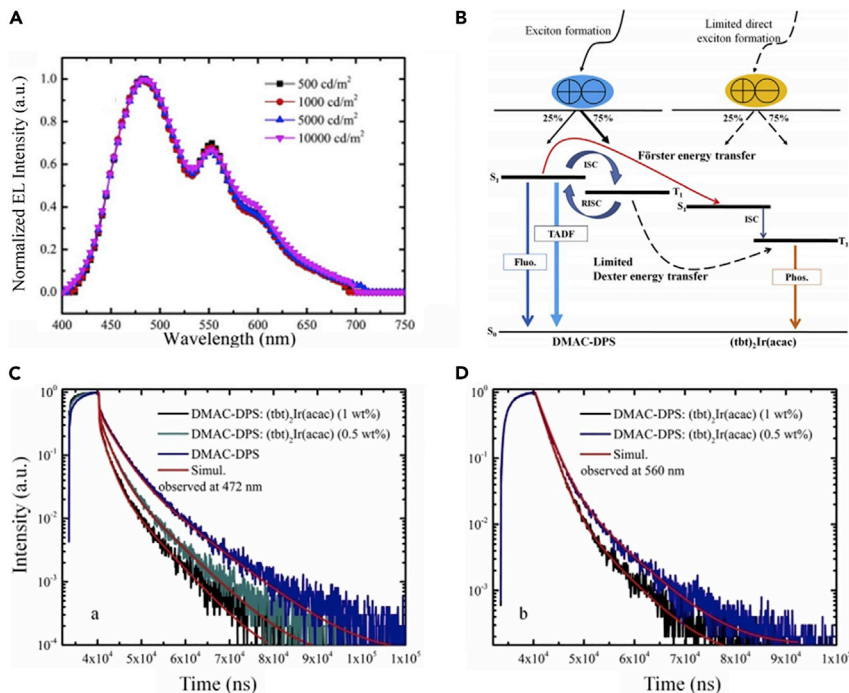


**Figure 21. EL spectra, light-emitting mechanism, and PL transient decay characteristics diagrams**

(A–D) (A) The normalized EL spectra for the optimized hybrid white OLED; (B) Schematic EL mechanism diagram of DMAC-DPS and  $(\text{tbt})_2\text{Ir}(\text{acac})$  in hybrid white OLED; Experimental and simulated PL transient decay characteristics of the DMAC-DPS neat film and DMAC-DPS:  $(\text{tbt})_2\text{Ir}(\text{acac})$  blend films with doping concentrations of 0.5 wt % and 1 wt % observed at 472 nm (C) and 560 nm (D) under nitrogen atmosphere. Reproduced with permission (Qi et al., 2017a), Copyright, Elsevier.

TADF emitters are insensitive to the doping ratio, enabling high-efficiency OLEDs using non-doped technology. All above advantages indicate blue TADF emitters are more suitable for building simple and high performance hybrid white OLEDs.

In this respect, a sky-blue TADF emitter DMAC-DPS first caught the eye of researchers because of its high  $T_1$  level (2.9 eV) and PLQY (0.88) in neat film. In addition, DMAC-DPS also exhibits a broad emission spectrum with a full width at half maximum of about 80 nm (Wang et al., 2017; Zhao et al., 2017). Thus, in 2017, Yu et al. firstly inserted an orange phosphorescent UEML in a blue TADF EML structured by heavily doping DMAC-DPS in DPEPO host, to fabricate complementary hybrid white OLEDs (Qi et al., 2017a), and the optimized device structure is ITO/  $\text{MoO}_3$ (10 nm)/ TAPC(40 nm)/ mCP(10 nm)/ DPEPO: 50wt% DMAC-DPS(9 nm)/  $(\text{tbt})_2\text{Ir}(\text{acac})(0.1 \text{ nm})$ / DPEPO: 50wt% DMAC-DPS(6 nm)/ Bphen(40 nm)/ Mg: Ag (100 nm). The hybrid white OLED obtains the peak PE and EQE of 45.8 lm W<sup>-1</sup> and 15.7%, and shows a stable EL spectra with slight CIE coordinates shift of (0.008, 0.003) with luminance increasing from 1000 to 10,000 cd m<sup>-2</sup>, as shown in Figure 21A. The PL transient decay characteristics manifest that a fraction of  $(\text{tbt})_2\text{Ir}(\text{acac})$  phosphorescence originated from triplet excitons on DMAC-DPS via up conversion and the whole light-emitting mechanism is dominated by Förster energy transfer, which ensures a stable EL spectra, as shown in Figures 21B–21D.

In 2018, Ma et al. further proved the superiority of blue TADF material of DMAC-DPS in the development of hybrid white OLEDs. They strategically inserted phosphorescent green and red UEMLs in appropriate positions in blue TADF DMAC-DPS layer to obtain highly efficient, low efficiency roll-off, and high CRI hybrid white OLEDs with the structure of ITO(180 nm)/ $\text{MoO}_3$ (8 nm)/TAPC: 15wt% $\text{MoO}_3$ (50 nm)/ TAPC(10 nm)/ mCP(10 nm)/ DMAC-DPS(7.5 nm)/ Ir(MDQ)<sub>2</sub>(acac)(0.03 nm)/ DMAC-DPS(2.5 nm)/ Ir(ppy)<sub>2</sub>(acac)(0.09 nm)/ DMAC-DPS(2.5 nm)/ Ir(MDQ)<sub>2</sub>(acac)(0.03 nm)/ DMAC-DPS(7.5 nm)/ DPEPO(5 nm)/ BmPyPB: 3wt% $\text{Li}_2\text{CO}_3$ (35 nm)/  $\text{Li}_2\text{CO}_3$ (1 nm)/Al. For example, the fabricated hybrid white OLED achieves the maximum CE, PE, and EQE of 41.6 cd A<sup>-1</sup>, 42.4 lm W<sup>-1</sup>, and 19.1%, respectively,

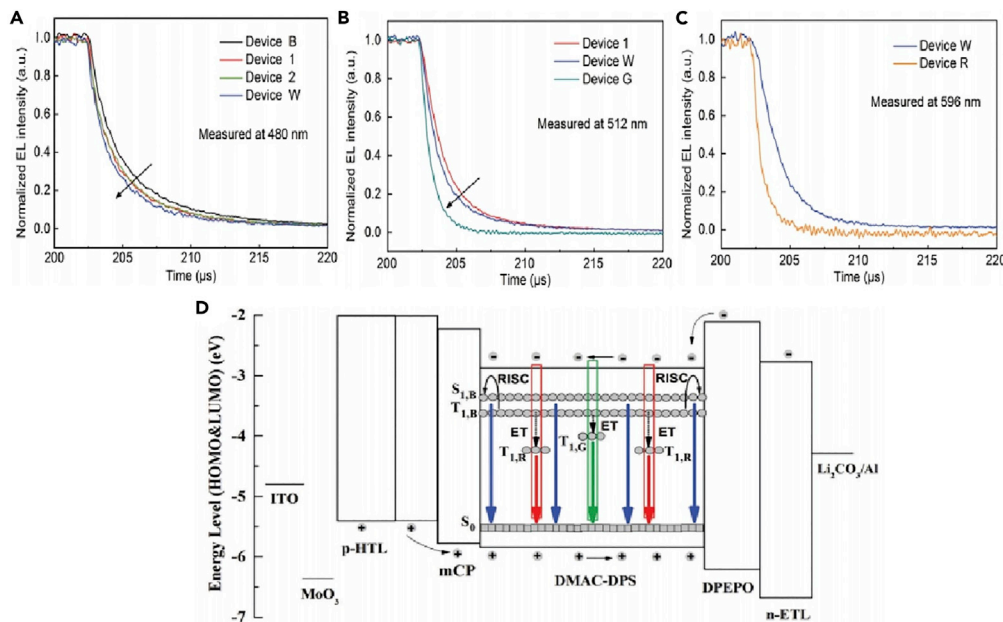


**Figure 22. Time-resolved EL decay of EML and energy level diagram of corresponding OLEDs**

The time-resolved EL decay curves measured at 480 nm (A), at 512 nm (B), and at 596 nm (C), and the structures of EMLs were DMAC-DPS(10 nm)/Ir(ppy)<sub>2</sub>(acac)(0.09 nm)/DMAC-DPS(10 nm) in Device 1, DMAC-DPS(7.5 nm)/Ir(MDQ)<sub>2</sub>(acac)(0.03 nm)/DMACDPS(5 nm)/Ir(ppy)<sub>2</sub>(acac)(0.03 nm)/DMAC-DPS(7.5 nm) in Device 2, TCTA:Ir(ppy)<sub>2</sub>(acac)(10 nm, 5%) in Device G, and TCTA:Ir(MDQ)<sub>2</sub>(acac)(10 nm, 5%) in Device R; (D) Proposed energy level diagram of the optimized white OLEDs. Reproduced with permission [Zhao et al., 2018a], Copyright, Royal Society of Chemistry.

(Zhao et al., 2018a), and at a luminance of 1000 cd m<sup>-2</sup>, the CE and EQE still retain 39.2 cd A<sup>-1</sup> and 17.3%, respectively. Besides, a high CRI of >80 is realized at a wide luminance range from 100 cd m<sup>-2</sup> to 10,000 cd m<sup>-2</sup>, which can satisfy practical applications. A series of transient EL decay curves measured at the wavelengths of 480 nm, 512 nm, and 596 nm, corresponding to the emission of DMAC-DPS, Ir(ppy)<sub>2</sub> acac, and Ir MDQ<sub>2</sub>(acac), are carried out (shown in Figures 22A–22C), clearly indicating the phosphorescent emission mechanism is originated from the energy transfer from DMAC-DPS to Ir(ppy)<sub>2</sub>(acac) or Ir MDQ<sub>2</sub>(acac) but direct trapping emission processes of phosphors, as shown Figure 22D. This can consume some triplet excitons generated at DMAC-DPS for high exciton utilization and reduced exciton quenching. For low efficiency roll-off, it is demonstrated that the main reason is the broadened carrier recombination zone across the whole EML by bipolar DMAC-DPS emitter. Actually, when they replaced the blue TADF emitter with a co-doping forming blue exciplex having similar bipolar transport and TADF characteristics, the prepared hybrid white OLED realized slightly better EL performance, revealing the universality of the proposed EML structure composed of blue TADF emitter and long-wavelength phosphorescent UEMLS.

Apart from DMAC-DPS, there are also other TADF emitters such reported using in hybrid white OLEDs, and the relevant devices also reveal high EL performance (Mu et al., 2020). For example, in 2018, 2CzPN employed as blue TADF emitter was introduced by Wang et al. to structure hybrid white OLEDs, where a yellow phosphorescent UEML of PO-01-TB was inserted in 2CzPN-doped blue fluorescent layer with the structure of ITO/HAT-CN(5 nm)/TAPC(40 nm)/TCTA(10 nm)/mCP:10 wt%2CzPN(15-day nm)/PO-01-TB(0.1 nm)/ mCP: 10wt%2CzPN(d nm) / B3PyMPM(50 nm) / LiF(0.8 nm)/Al (Dong et al., 2018). The formation of mCP/B<sub>3</sub>PyMPM-based interface exciplex guarantees the efficient triplet harvesting from exciplex by RISC, and the energy of exciplex is also transferred to blue TADF 2CzPN or yellow phosphors, as well as the energy transfer from blue fluorophors to yellow phosphors, contributing to white emission. Thus, the final white device (d = 3) achieved the high maximum CE, PE, and EQE of 65.9 cd A<sup>-1</sup>, 79.2 lm W<sup>-1</sup>, and 22.3%, respectively, further demonstrating the potential of blue TADF emitters in developing hybrid white OLEDs.

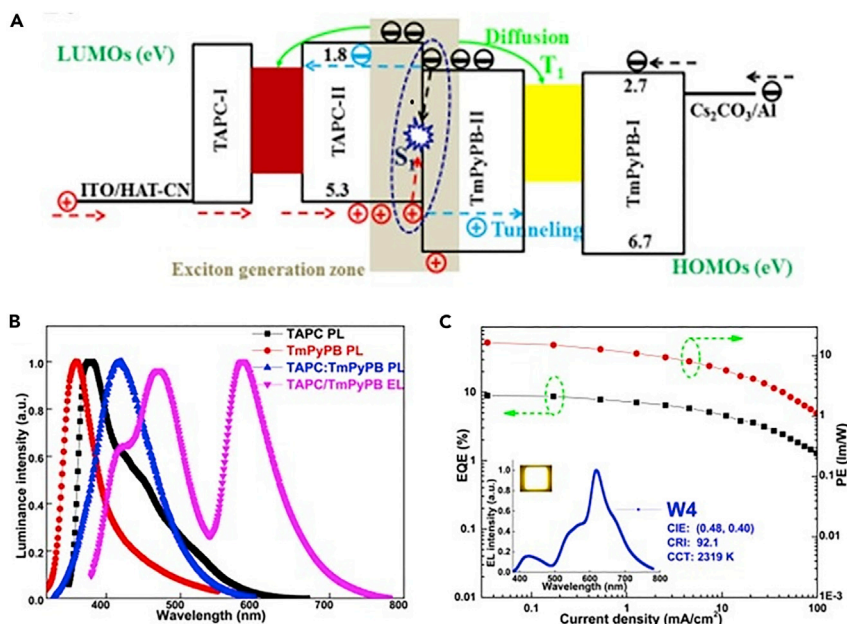


**Figure 23. Schematic emission mechanisms and EL performance diagrams**

(A–C) (A) Schematic emission mechanisms of the hybrid white OLEDs combining exciplex/electroplex with broad emission spectrum and red and yellow phosphorescent UEMls; (B) PL spectra of TAPC, TmPyPB, and TAPC:TmPyPB(1:1) mixed films, coupled with EL spectrum of device W1 with the structure of ITO/HAT-CN (100 nm)/TAPC (25 nm)/TmPyPB (35 nm)/Cs<sub>2</sub>CO<sub>3</sub> (1 nm)/Al (160 nm); (C) EQE-J-PE characteristic curve of above target hybrid white OLED, and the inset is the photograph and spectrum at 1000 cd m<sup>-2</sup> for target device. Reproduced with permission (Luo et al., 2017), Copyright, American Chemical Society.

### Phosphorescent UEMls inserted into blue exciplex EML

In addition to TADF molecules of intramolecular charge-transfer mechanism as mentioned above, exciplex or intermolecular charge-transfer mechanism can also realize the 100% utilization of excitons, bipolar transport character, and broad blue fluorescent emission (Ban et al., 2019; Guo et al., 2021). Hence, we also carefully reviewed some relevant research that combines blue exciplex with phosphorescent UEMls to design hybrid white OLEDs. In earlier studies, the exciplex-based white OLEDs have not received enough attention because of the poor efficiency of exciplex. With the understanding of the TADF process, the EL performances of exciplex-based devices have been significantly enhanced, promoting the application of exciplex in white OLEDs (Xiao et al., 2018). It is deserved to point out that not all exciplexes have TADF character, but all exciplexes can be used to develop hybrid white OLED, regardless of with TADF or without TADF character.

In 2017, Liu et al. verified TAPC:TmPyPB-forming exciplex by a new red-shifted PL emission with the peak of 421 nm compared to the PL spectra of pure TAPC and TmPyPB films. Surprisingly, the EL spectra for TAPC/TmPyPB-based bilayer device exhibits distinct emission peaks (425, 468, and 585 nm), where the low-energy peaks (468 and 585 nm) have not been recorded from the PL spectrum, which are originated from the electroplexes that only occur under the electric excitation, as shown in Figure 23B. Such a broad emission spectrum is very advantageous to construct white OLEDs. Thus, they inserted red and yellow phosphorescent UEMls in donor and acceptor layers on either side of interfacial exciplex of TAPC/TmPyPB and some distance away from TAPC/TmPyPB interface, to develop three color hybrid white OLED with the structure of ITO/ HAT-CN(100 nm)/ TAPC(22 nm)/ Ir(piq)<sub>3</sub>(0.3 nm)/ TAPC(3 nm)/ TmPyPB(20 nm)/ Ir(dmppy)<sub>2</sub>(dpp)(0.3 nm)/TmPyPB(35 nm)/Cs<sub>2</sub>CO<sub>3</sub>(1 nm)/Al(160 nm) (Luo et al., 2017). Charges accumulated at TAPC/TmPyPB interface, ensuring exciplex formation for effective exciplex/electroplex-based broad spectral emission. At the same time, a few excitons formed on TAPC and TmPyPB and lots of exciplex triplet excitons transfer energy to phosphorescent UEMls on both sides of exciplex for strong red and yellow light emissions, and they combine with above exciplex/electroplex emission to produce high color quality white light emission (Figure 23A). Consequently, the target device exhibits a

high very high CRI of 92.1 and a low CCT of 2319 K, as shown in Figure 23C. However, the device efficiency is relatively low with maximum EQE only reaching 15.1% owing to inefficient blue exciplex without TADF character.

Selecting more effective blue exciplex with TADF characteristic, several highly efficient hybrid white OLEDs were reported by incorporating phosphorescent UEMs into blue exciplex layers (Wang et al., 2018; Zhao et al., 2019; Ying et al., 2018a). A representative achievement is that the peak PE and EQE of 97.1 lm W<sup>-1</sup> and 22.45% for hybrid white OLED were accomplished by Ma et al., in 2018 (Ying et al., 2018a). They proposed the detailed device structure is ITO/ HAT-CN(15 nm)/ TAPC(60 nm)/ TCTA(5 nm)/ mCBP(5 nm)/ mCBP:PO-T2T(1:1, 3 nm)/ Ir(tptpy)<sub>2</sub>(acac)(0.05 nm)/ mCBP: PO-T2T(1:1, 12 nm)/ PO-T2T(45 nm)/ Liq(1.5 nm)/ Al (150 nm), in which EML is simply formed with a 0.05 nm-thick orange UEM of Ir(tptpy)<sub>2</sub>(acac) incorporated into blue bulk exciplex of mCBP: PO-T2T. On this basis, using the same blue exciplex, they doped blue phosphor Flpic in blue exciplex mCBP: PO-T2T and implanted orange and green phosphorescent UEMs in the suitable position of blue phosphor-doped exciplex layer to further develop three color hybrid white OLEDs. In addition, the detailed structure is ITO/HAT-CN (15 nm)/ TAPC(60 nm)/ TCTA(5 nm)/ mCBP(5 nm)/ mCBP:PO-T2T:Flpic (1:1:10wt%, 7 nm)/ Ir(ppy)<sub>2</sub>(acac)(0.03 nm)/ mCBP:PO-T2T:Flpic(1:1:10wt%, 2 nm)/ Ir(tptpy)<sub>2</sub>(acac)(0.07 nm)/ mCBP:PO-T2T:Flpic (1:1:10wt%, 6 nm)/ PO-T2T(45 nm)/Liq(1.5 nm)/ Al(150 nm) (Ying et al., 2018b). Exhilaratingly, not only a lower turn-on voltage of 2.3 V and higher efficiency with EQE reaching 22.8% are obtained, but efficiency roll-off is also effectively suppressed for the fabricated hybrid white OLED. For example, at a practical luminance of 1000 and 5000 cd m<sup>-2</sup>, the EQEs are still up to 21.9 and 20.4%, respectively. To the best of our knowledge, these are among the best efficiencies for hybrid white OLED under such high luminance. Such low turn-on voltage could be ascribed to the high carrier mobility of exciplex donor (TAPC) and acceptor (PO-T2T) as well as the charge “barrier-free” injection from charge-transporting layers into the EML. In addition, the effectively reduced efficiency roll-off is believed to be broadened carrier recombination zone by blue bulk exciplex and decreased exciton density derived from strategically managing triplet excitons by introducing phosphorescent UEMs way. Above outstanding work demonstrated it should be a very promising avenue for designing and developing simplified but high performance white OLEDs by combining blue TADF exciplex and phosphorescent UEMs.

## CONCLUSIONS AND OUTLOOK

It is demonstrated that molecules of UEMs (<1 nm) are not in the form of a neat layer but partially penetrate the adjacent layers with few island-like structures, which can be considered to be doped in two-dimensional form compare to the conventional doping method with hosts and dopants mixed in three-dimensional form. Thus, UEMs is a special form of doping emitters without co-doping process, which can effectively simplify device structure and preparation process, and offer more flexible design for device structure and lower material consumption. Due to above special structure, it is found that the introduction of UEMs doesn't significantly affect the carrier behavior of devices, where the carriers directly captured by UEMs are almost negligible, and most excitons used for molecular radiative transition are still derived from the diffusion and energy transfer of main recombination zone. Hence, the EL mechanism in UEMs-based OLEDs is still mainly dominated by host-guest energy transfer. Compared to the conventional doped EMLs, it is found that UEMs also show a similar PL spectrum, PLQY, and emitter orientation, implying that molecular aggregation, which would be detrimental for the performance, is negligible. This is beneficial for reducing molecular aggregation, eliminating concentration quenching, and contributing to complete exciton utilization.

Based on the advantages of UEMs mentioned above, phosphorescent dyes forming UEMs have been actively investigated in the monochromatic and white OLEDs in recent years. In addition, the resulting OLEDs based on UEMs achieved high EL performance comparable to the conventional doping-based devices, confirming the effectiveness of UEMs structure. To sum up, phosphorescent UEMs are mainly inserted into nonluminous materials (single material and mixed materials), heterojunction interface (without and with exciplex formation) as well as into luminescent materials (phosphorescent, conventional fluorescent, TADF, and exciplex emitters) for structuring OLEDs. Among them, phosphorescent UEMs are first sandwiched between nonluminous materials, in which it was verified the spacer, acting as the carrier or exciton adjusting layer, has a very important influence on device performance. When the spacer is formed by doped a hole transport material into an electron transport material, i.e., mixed spacer,

especially when mixed spacer form exciplex, can effectively reduce charge injection barrier, balance charge carrier transport, and extend exciton recombination zone, which is beneficial for obtaining higher device performance. To further simplify device structure, phosphorescent UEMs are directly introduced into the heterojunction interface, which is the main carrier recombination zone. It was demonstrated that such a device can almost completely utilize all carriers and excitons at the interface, and be successfully applied in inverted and tandem OLEDs, realizing high maximum efficiency comparable to the conventional doped-EMs device. However, the high excitons concentration at the heterojunction interface easily causes excitons quenching, inducing severe efficiency roll-off. Thus, UEMs are also incorporated into heterojunction interface with exciplex formation or some distance away from the interface, can effectively dilute the excitons concentration in UEMs, which is proved to be a very effective method for improving efficiency roll-off. But, it may not be suitable for structuring high color quality white OLEDs because such devices require the introduction of more heterojunction interface matched to more complementary UEMs, seriously complicating device structure. To develop white OLEDs, to directly insert long wavelength phosphorescent UEMs into blue light-emitting zones is a very simple and promising approach. Among them, using blue fluorophores and complementary phosphorescent UEMs, the structured hybrid white OLEDs have drawn considerable attention due to their advantages of simultaneously combining the excellent stability of blue fluorophors and the high efficiency of long wavelength phosphors. The precise arrangement of thickness and insertion position for UEMs in blue fluorescent EML demonstrated a series of simplified, highly efficient, and high color quality white OLEDs. In addition, a rich selection of high performance blue fluorophore also gives a more flexible design for white OLEDs. Recently developed TADF emitters are considered as promising alternatives to replace the conventional blue fluorescent emitters in OLEDs. Compared with the conventional blue fluorescent emitters, the high  $T_1$ , high efficiency and good bipolar transport for blue TADF emitters, and exciplex with TADF character make them become more suitable blue fluorescent emitters combined with phosphorescent UEMs in developing hybrid white OLEDs. In addition, such hybrid white OLEDs have become the focus of recent research, and also achieve higher device efficiency due to more efficient energy transfer and exciton utilization. Nevertheless, the lack of efficient TADF materials with deep blue emission also become a limiting factor for further development of such hybrid white OLEDs.

Look forward to the future, simplifying the structure and reducing the cost will be still the core factors to promote the further large-scale industrialization of OLEDs. In this respect, UEMs exhibit unique advantages and potential. We believe UEMs will be more widely used in the structure design and device preparation of OLEDs. Especially for the development of white OLEDs, the hybrid white OLEDs, simultaneously combining phosphorescent UEMs with blue fluorophores (conventional fluorescent, TADF, and exciplex emitters) maybe become the mainstream. Herein, various blue fluorophors (conventional fluorescent, TADF, and exciplex emitters) with high PLQY, high  $T_1$  level, and excellent bipolar transport characteristics are still crucial for structuring simplified but high-performance hybrid white OLEDs. Thus, it is still the main research direction to design and synthesize higher performance blue fluorescent material, to accurately regulate the thickness and insertion position of UEMs for device fabrication and to reveal the underlying energy transfer and light emitting mechanism between excitons generated in UEMs and blue fluorophores for complete exciton utilization. We expect and believe a series of encouraging research achievements can be completed in UEMs-based OLEDs in the future.

## ACKNOWLEDGMENTS

The authors acknowledge financial support from National Natural Science Foundation of China (61705156), Key R&D program of Shanxi Province (International Cooperation, 201903D421087), Shanxi-Zheda Institute of Advanced Materials and Chemical Engineering (2021SX-FR007), and Program for the Innovative Talents of Higher Education Institutions of Shanxi.

## AUTHOR CONTRIBUTIONS

Y.M. worked on the conceptualization of the paper frame. The original draft was written by M.Y. The paper was further edited by Y.M.

## DECLARATION OF INTERESTS

The authors declare no competing interests.

REFERENCES

- Ban, X.X., Liu, Y., Pan, J., Chen, F., Zhu, A.Y., Jiang, W., Sun, Y.M., and Dong, Y.J. (2019). Design of blue thermally activated delayed fluorescent emitter with efficient exciton gathering property for high-performance fully solution-processed hybrid white OLEDs. *ACS Appl. Mater. Inter.* 12, 1190–1200.
- Byeon, S.Y., Lee, D.R., Yook, K.S., and Lee, J.Y. (2019). Recent progress of singlet-exciton-harvesting fluorescent organic light-emitting diodes by energy transfer processes. *Adv. Mater.* 31, 1803714.
- Chen, D.C., Liu, K.K., Gan, L., Liu, M., Gao, K., Xie, G.Z., Ma, Y.G., Cao, Y., and Su, S.J. (2016a). Modulation of exciton generation in organic active planar pn heterojunction: toward low driving voltage and high-efficiency OLEDs employing conventional and thermally activated delayed fluorescent emitters. *Adv. Mater.* 28, 6758–6765.
- Chen, P., Chen, B.Y., Zuo, L.M., Duan, Y., Han, G.G., Sheng, R., Xue, K.W., and Zhao, Y. (2016b). High-efficiency and superior color-stability white phosphorescent organic light-emitting diodes based on double mixed-host emission layers. *Org. Electron.* 31, 136–141.
- Chen, C., Liu, Y.F., Chen, Z., Wang, H.R., Wei, M.Z., Bao, C., Zhang, G., Gao, Y.H., Liu, C.L., Jiang, W.L., et al. (2017). High efficiency warm white phosphorescent organic light emitting devices based on blue light emission from a bipolar mixed-host. *Org. Electron.* 45, 273–278.
- Chen, Y.W., Ying, S.A., Sun, Q., Dai, Y.F., Qiao, X.F., Yang, D.Z., Chen, J.S., and Ma, D.G. (2018). High efficiency hybrid white organic light-emitting diodes based on a simple and efficient exciton regulation emissive layer structure. *RSC Adv.* 8, 40883–40893.
- Chen, Y.W., Sun, Q., Dai, Y.F., Yang, D.Z., Qiao, X.F., and Ma, D.G. (2019). EL properties and exciton dynamics of high-performance doping-free hybrid WOLEDs based on 4P-NPD/Bepp2 heterojunction as blue emitter. *Adv. Opt. Mater.* 7, 1900703.
- Chen, Y.W., Wu, Y.B., Lin, C.W., Dai, Y.F., Sun, Q., Yang, D.Z., Qiao, X.F., and Ma, D.G. (2020). Simultaneous high efficiency/CRI/spectral stability and low efficiency roll-off hybrid white organic light-emitting diodes via simple insertion of ultrathin red/green phosphorescent emitters in a blue exciplex. *J. Mater. Chem. C* 8, 12450–12456.
- Chen, H., Liu, H.J., Shen, P.C., Zeng, J.J., Jiang, R.M., Fu, Y., Zhao, Z.J., and Tang, B.Z. (2021). Efficient sky-blue bipolar delayed fluorescence luminogen for high-performance single emissive layer WOLEDs. *Adv. Opt. Mater.* 9, 2002019.
- Dai, X.D., and Cao, J. (2020). Study on spectral stability of white organic light-emitting diodes with mixed bipolar spacer based on ultrathin non-doped phosphorescent emitting layers. *Org. Electron.* 78, 105563.
- Dai, X.D., Yao, F.N., Li, J., Yu, H.J., and Cao, J. (2019). Color-stable non-doped white phosphorescent organic light-emitting diodes based on ultrathin emissive layers. *J. Phys. D Appl. Phys.* 53, 055106.
- D'Andrade, B.W., Holmes, R.J., and Forrest, S.R. (2004). Efficient organic electrophosphorescent white-light-emitting device with a triple doped emissive layer. *Adv. Mater.* 16, 624–628.
- Dong, H., Jiang, H.P., Wang, J.D., Guan, Y., Hua, J., Gao, X., Bo, B.X., and Wang, J. (2018). High-efficiency and color-stable warm white organic light-emitting diodes utilizing energy transfer from interface exciplex. *Org. Electron.* 62, 524–529.
- Gather, M.C., Köhnen, A., and Meerholz, K. (2011). White organic light-emitting diodes. *Adv. Mater.* 23, 233–248.
- Guo, J.F., Zhen, Y.G., Dong, H.L., and Hu, W.P. (2021). Recent progress on organic exciplex materials with different donor-acceptor contacting modes for luminescent applications. *J. Mater. Chem. C* 9, 16843–16858.
- Han, C., Zhang, J., Ma, P., Yang, W.B., and Xu, H. (2021). Host engineering based on multiple phosphorylation for efficient blue and white TADF organic light-emitting diodes. *Chem. Eng. J.* 405, 126986.
- Jeon, S.O., Lee, K.H., Kim, J.S., Ihn, S.G., Chung, Y.S., Kim, J.W., Lee, H., Kim, S., Choi, H., and Lee, J.Y. (2021). High-efficiency, long-lifetime deep-blue organic light-emitting diodes. *Nat. Photon.* 15, 208–215.
- Jou, J.H., Kumar, S., Agrawal, A., Li, T.H., and Sahoo, S. (2015). Approaches for fabricating high efficiency organic light emitting diodes. *J. Mater. Chem. C* 3, 2974–3002.
- Kang, J.S., Yoo, S.I., Kim, J.W., Yoon, G.J., Yi, S., and Kim, W.Y. (2016). Confinement of holes and electrons in blue organic light-emitting diodes with additional red emissive layers. *Opt. Mater.* 52, 181–185.
- Kang, S.W., Baek, D.H., Ju, B.K., and Park, Y.W. (2021). Green phosphorescent organic light-emitting diode exhibiting highest external quantum efficiency with ultra-thin undoped emission layer. *Sci. Rep.* 11, 1–8.
- Kim, K.H., Moon, C.K., Lee, J.H., Kim, S.Y., and Kim, J.J. (2014). Highly efficient organic light-emitting diodes with phosphorescent emitters having high quantum yield and horizontal orientation of transition dipole moments. *Adv. Mater.* 26, 3844–3847.
- Lee, S.H., Kim, K.H., Limbach, D., Park, Y.S., and Kim, J.J. (2013). Low roll-off and high efficiency orange organic light emitting diodes with controlled co-doping of green and red phosphorescent dopants in an exciplex forming co-host. *Adv. Funct. Mater.* 23, 4105–4110.
- Lee, S., Shin, H., and Kim, J.J. (2014a). High-efficiency orange and tandem white organic light-emitting diodes using phosphorescent dyes with horizontally oriented emitting dipoles. *Adv. Mater.* 26, 5864–5868.
- Lee, S., Lee, S., Yoo, S.J., Kim, K.H., and Kim, J.J. (2014b). Langevin and trap-assisted recombination in phosphorescent organic light emitting diodes. *Adv. Funct. Mater.* 24, 4681–4688.
- Li, Y.C., Li, X.L., Chen, D.J., Cai, X.Y., Xie, G.Z., He, Z.Z., Wu, Y.C., Lien, A., Cao, Y., and Su, S.J. (2016). Design strategy of blue and yellow thermally activated delayed fluorescence emitters and their all-fluorescence white OLEDs with external quantum efficiency beyond 20%. *Adv. Funct. Mater.* 26, 6904–6912.
- Li, S.H., Wu, S.F., Wang, Y.K., Liang, J.J., Sun, Q., Huang, C.C., Wu, J.C., Liao, L.S., and Fung, M.K. (2018). Management of excitons for highly efficient organic light-emitting diodes with reduced triplet exciton quenching: synergistic effects of exciplex and quantum well structure. *J. Mater. Chem. C* 6, 342–349.
- Li, Y., Li, Z., Zhang, J., Han, C.M., Duan, C.B., and Xu, H. (2021). Manipulating complementarity of binary white thermally activated delayed fluorescence systems for 100% exciton harvesting in OLEDs. *Adv. Funct. Mater.* 31, 2011169.
- Liao, X.Q., An, K., Cheng, J., Li, Y., Meng, X., Yang, X., and Li, L. (2019). High efficiency ultra-thin doping-free WOLED based on blue thermally activated delayed fluorescence inter-layer switch. *Appl. Surf. Sci.* 487, 610–615.
- Lin, R., Wang, F., Rybicki, J., Wohlgemuth, M., and Hutchinson, K.A. (2010). Distinguishing between tunneling and injection regimes of ferromagnet/organic semiconductor/ferromagnet junctions. *Phys. Rev. B* 81, 195214.
- Liu, S.Q., Yu, J.S., Ma, Z., and Zhao, J. (2013a). Highly efficient white organic light-emitting devices consisting of undoped ultrathin yellow phosphorescent layer. *J. Lumines.* 134, 665–669.
- Liu, B.Q., Xu, M., Wang, L., Su, Y.J., Gao, D.Y., Tao, H., Lan, L.F., Zou, J.H., and Peng, J.B. (2013b). High-performance hybrid white organic light-emitting diodes comprising ultrathin blue and orange emissive layers. *Appl. Phys. Express* 6, 122101.
- Liu, J., Shi, X.D., Wu, X.K., Wang, J., Min, Z.Y., Wang, Y., Yang, M.J., Chen, C.H., and He, G.F. (2014). Achieving above 30% external quantum efficiency for inverted phosphorescence organic light-emitting diodes based on ultrathin emitting layer. *Org. Electron.* 15, 2492–2498.
- Liu, B.Q., Wang, L., Gao, D.Y., Xu, M., Zhu, X.H., Zou, J.H., Lan, L.F., Ning, H.L., Peng, J.B., and Cao, Y. (2015). Harnessing charge and exciton distribution towards extremely high performance: the critical role of guests in single-emitting-layer white OLEDs. *Mater. Horiz.* 2, 536–544.
- Liu, B.Q., Tao, H., Wang, L., Gao, D.Y., Liu, W.C., Zou, J.H., Xu, M., Ning, H.L., Peng, J.B., and Cao, Y. (2016). High-performance doping-free hybrid white organic light-emitting diodes: the exploitation of ultrathin emitting nanolayers (< 1 nm). *Nano Energy* 26, 26–36.
- Liu, B.Q., Nie, H., Lin, G.W., Hu, S.B., Gao, D.Y., Zou, J.H., Xu, M., Wang, L., Zhao, Z.J., Ning, H.L., et al. (2017). High-performance doping-free hybrid white OLEDs based on blue aggregation-induced emission luminogens. *ACS Appl. Mater. Inter.* 9, 34162–34171.
- Liu, Y., Hänsch, C., Wu, Z., Will, P.A., Fries, F., Wu, J., Lenk, S., Leo, K., and Reineke, S. (2019).

Locking excitons in two-dimensional emitting layers for efficient monochrome and white organic light-emitting diodes. *J. Mater. Chem. C* 7, 8929–8937.

Liu, H., Liu, F.T., and Lu, P. (2020). Multiple strategies towards high-efficiency white organic light-emitting diodes by the vacuum deposition method. *J. Mater. Chem. C* 8, 5636–5661.

Luo, D.X., Li, X.L., Zhao, Y., Gao, Y., and Liu, B.Q. (2017). High-performance blue molecular emitter-free and doping-free hybrid white organic light-emitting diodes: an alternative concept to manipulate charges and excitons based on exciplex and electropolymer emission. *ACS Photon.* 4, 1566–1575.

Luo, D.X., Chen, Q.Z., Gao, Y., Zhang, M.L., and Liu, B.Q. (2018). Extremely simplified, high-performance, and doping-free white organic light-emitting diodes based on a single thermally activated delayed fluorescent emitter. *ACS Energy Lett.* 3, 1531–1538.

Luo, D.X., Xiao, P., and Liu, B.Q. (2019). Doping-free white organic light-emitting diodes. *Chem. Rec.* 19, 1596–1610.

Ma, Z., Zhou, S.L., Hu, S., and Yu, J.S. (2014). Recombination region improvement for reduced efficiency roll-off in phosphorescent OLEDs with dual emissive layers. *J. Lumines.* 154, 376–380.

Meng, L.Q., Wang, H., Wei, X.F., Liu, J.J., Chen, Y.Z., Kong, X.B., Lv, X.P., Wang, P.F., and Wang, Y. (2016). Highly efficient nondoped organic light emitting diodes based on thermally activated delayed fluorescence emitter with quantum-well structure. *ACS Appl. Mater. Inter.* 8, 20955–20961.

Miao, Y.Q., Zhao, B., Gao, Z.X., Shi, H.P., Tao, P., Wu, Y.L., Wang, K.X., Wang, H., Xu, B.S., and Zhu, F.R. (2017a). A novel intramolecular charge transfer blue fluorophor for high color stability hybrid di-chromatic white organic light-emitting diodes. *Org. Electron.* 42, 1–7.

Miao, Y.Q., Wang, K.X., Zhao, B., Gao, L., Wang, Y.W., Wang, H., Xu, B.S., and Zhu, F.R. (2017b). Manipulation and exploitation of singlet and triplet excitons for hybrid white organic light-emitting diodes with superior efficiency/CRI/color stability. *J. Mater. Chem. C* 5, 12474–12482.

Miao, Y.Q., Tao, P., Wang, K.X., Li, H.X., Zhao, B., Gao, L., Wang, H., Xu, B.S., and Zhao, Q. (2017c). Highly efficient red and white organic light-emitting diodes with external quantum efficiency beyond 20% by employing pyridylimidazole-based metallophosphors. *ACS Appl. Mater. Inter.* 9, 37873–37882.

Miao, Y.Q., Tao, P., Gao, L., Li, X.L., Wei, L.W., Liu, S.J., Wang, H., Xu, B.S., and Zhao, Q. (2018a). Highly efficient chlorine functionalized blue iridium (III) phosphors for blue and white phosphorescent organic light-emitting diodes with the external quantum efficiency exceeding 20%. *J. Mater. Chem. C* 6, 6656–6665.

Miao, Y.Q., Wang, K.X., Gao, L., Zhao, B., Wang, H., Zhu, F.R., Xu, B.S., and Ma, D.G. (2018b). Precise manipulation of the carrier recombination zone: a universal novel device structure for highly efficient monochrome and white phosphorescent organic light-emitting diodes with extremely small efficiency roll-off. *J. Mater. Chem. C* 6, 8122–8134.

Miao, Y.Q., Wang, K.X., Zhao, B., Gao, L., Tao, P., Liu, X.G., Hao, Y.Y., Wang, H., Xu, B.S., and Zhu, F.R. (2018c). High-efficiency/CRI/color stability warm white organic light-emitting diodes by incorporating ultrathin phosphorescence layers in a blue fluorescence layer. *Nanophotonics* 7, 295–304.

Miao, Y.Q., Wang, K.X., Gao, L., Wang, H., Zhu, F.R., and Xu, B.S. (2018d). Non-phosphor-doped fluorescent/phosphorescent hybrid white organic light-emitting diodes with a sandwiched blue emitting layer for simultaneously achieving superior device efficiency and color quality. *J. Mater. Chem. C* 6, 9811–9820.

Miao, Y.Q., Wang, K.X., Gao, L., Zhao, B., Wang, Z.Q., Zhao, Y.P., Zhang, A.Q., Wang, H., Hao, Y.Y., and Xu, B.S. (2018e). Combining emissions of hole-and electron-transporting layers simultaneously for simple blue and white organic light-emitting diodes with superior device performance. *J. Mater. Chem. C* 6, 1853–1862.

Miao, Y.Q., Wei, X.Z., Gao, L., Wang, K.X., Zhao, B., Wang, Z.Q., Zhao, B., Wang, H., Wu, Y.C., and Xu, B.S. (2019). Tandem white organic light-emitting diodes stacked with two symmetrical emitting units simultaneously achieving superior efficiency/CRI/color stability. *Nanophotonics* 8, 1783–1794.

Mu, H.C., Jiang, Y.X., and Xie, H.F. (2019). Efficient blue phosphorescent organic light emitting diodes based on exciplex and ultrathin Firpic sandwiched layer. *Org. Electron.* 66, 195–205.

Mu, H.C., Yao, M.Q., Wang, R.B., Qian, M., Xie, H.F., and Wang, D.S. (2020). White organic light emitting diodes based on localized surface plasmon resonance of Au nanoparticles and neat thermally activated delayed fluorescence and phosphorescence emission layers. *J. Lumines.* 220, 117022.

Park, M.J., Son, Y.H., Yang, H.I., Kim, S.K., Lampande, R., and Kwon, J.H. (2018). Optical design and optimization of highly efficient sunlight-like three-stacked warm white organic light emitting diodes. *ACS Photon.* 5, 655–662.

Pode, R. (2020). Organic light emitting diode devices: an energy efficient solid state lighting for applications. *Renew. Sust. Energy Rev.* 133, 110043.

Qi, Y.G., Wang, Z.J., Hou, S.H., and Yu, J.S. (2017a). Color stable and highly efficient hybrid white organic light-emitting devices using heavily doped thermally activated delayed fluorescence and ultrathin non-doped phosphorescence layers. *Org. Electron.* 43, 112–120.

Qi, Y.G., Hou, S.H., Li, J., Guo, H., and Yu, J.S. (2017b). Highly efficient organic light-emitting devices employing an ultrathin non-doped phosphorescence emitter within a thermally activated delayed fluorescence interface exciplex. *J. Lumines.* 192, 1242–1249.

Reineke, S., Lindner, F., Schwartz, G., Seidler, N., Walzer, K., Lüssem, B., and Leo, K. (2009). White organic light-emitting diodes with fluorescent tube efficiency. *Nature* 459, 234–238.

Schwartz, G., Reineke, S., Rosenow, T.C., Walzer, K., and Leo, K. (2009). Triplet harvesting in hybrid

white organic light-emitting diodes. *Adv. Funct. Mater.* 19, 1319–1333.

Sheng, R., Zuo, L.M., Xue, K.W., Duan, Y., Chen, P., Cheng, G., and Zhao, Y. (2016). Efficient white phosphorescent organic light-emitting diodes consisting of orange ultrathin and blue mixed host emission layers. *J. Phys. D-appl. Phys.* 49, 335101.

Sheng, R., Song, J., Li, A., Zhang, F.J., Zhang, H., Duan, Y., Zheng, J., Wang, Z.M., and Chen, P. (2019). High-efficiency and low efficiency roll-off in white organic light-emitting diodes employing a novel blue emitter. *Org. Electron.* 75, 105375.

Sheng, R., Li, A., Zhang, F.J., Song, J., Duan, Y., and Chen, P. (2020). Highly efficient, simplified monochrome and white organic light-emitting devices based on novel exciplex host. *Adv. Opt. Mater.* 8, 1901247.

Shi, X.D., Liu, J., Wang, J., Wu, X.K., Zheng, Y.X., and He, G.F. (2014). High efficiency green phosphorescent top-emitting organic light-emitting diode with ultrathin non-doped emissive layer. *Org. Electron.* 15, 2408–2413.

Shih, C.J., Lee, C.C., Chen, Y.H., Biring, S., Kumar, G., Yeh, T.H., Sen, S., Liu, S.W., and Wong, K.T. (2018). Exciplex-forming cohost for high efficiency and high stability phosphorescent organic light-emitting diodes. *ACS Appl. Mater. Inter.* 10, 2151–2157.

Shin, H., Lee, S., Kim, K.H., Moon, C.K., Yoo, S.J., Lee, J.H., and Kim, J.J. (2014). Blue phosphorescent organic light-emitting diodes using an exciplex forming co-host with the external quantum efficiency of theoretical limit. *Adv. Mater.* 26, 4730–4734.

Sun, N., Wang, Q., Zhao, Y.B., Chen, Y.H., Yang, D.Z., Zhao, F.C., Chen, J.S., and Ma, D.G. (2014). High-performance hybrid white organic light-emitting devices without interlayer between fluorescent and phosphorescent emissive regions. *Adv. Mater.* 26, 1617–1621.

Tan, T., Ouyang, S., Xie, Y.T., Wang, D.P., Zhu, D.L., Xu, X., and Fong, H.H. (2015). Balanced white organic light-emitting diode with non-doped ultra-thin emissive layers based on exciton management. *Org. Electron.* 25, 232–236.

Tang, X., Liu, X.Y., Yuan, Y., Wang, Y.J., Li, H.C., Jiang, Z.Q., and Liao, L.S. (2018). High-efficiency white organic light-emitting diodes integrating gradient exciplex allocation system and novel D-spiro-A materials. *ACS Appl. Mater. Inter.* 10, 29840–29847.

Tao, P., Miao, Y.Q., Zhang, Y.B., Wang, K.X., Li, H.X., Li, L., Li, X.L., Yang, T.T., Zhao, Q., Wang, H., et al. (2017). Highly efficient thiénylquinoline-based phosphorescent iridium (III) complexes for red and white organic light-emitting diodes. *Org. Electron.* 45, 293–301.

Tian, Q.S., Zhang, L., Hu, Y., Yuan, S., Wang, Q., and Liao, L.S. (2018). High-performance white organic light-emitting diodes with simplified structure incorporating novel exciplex-forming host. *ACS Appl. Mater. Inter.* 10, 39116–39123.

Tian, Q.S., Yuan, S., Shen, W.S., Zhang, Y.L., Wang, X.Q., Kong, F.C., and Liao, L.S. (2020). Multichannel effect of triplet excitons for highly

efficient green and red phosphorescent OLEDs. *Adv. Opt. Mater.* 8, 2000556.

Wang, Z.H., and Su, S.J. (2019). Molecular and device design strategies for ideal performance white organic light-emitting diodes. *Chem. Rec.* 19, 1518–1530.

Wang, X., Yu, J.S., Zhao, J., and Lei, X. (2012). Comparison of electron transporting layer in white OLED with a double emissive layer structure. *Displays* 33, 191–194.

Wang, Q., Oswald, I.W., Perez, M.R., Jia, H.P., Shahub, A.A., Qiao, Q.Q., Gnade, B.E., and Omary, M.A. (2014). Doping-free organic light-emitting diodes with very high power efficiency, simple device structure, and superior spectral performance. *Adv. Funct. Mater.* 24, 4746–4752.

Wang, J.X., Chen, J.S., Qiao, X.F., Alshehri, S.M., Ahamad, T., and Ma, D.G. (2016). Simple-structured phosphorescent warm white organic light-emitting diodes with high power efficiency and low efficiency roll-off. *ACS Appl. Mater. Inter.* 8, 10093–10097.

Wang, Z.J., Zhao, J., Zhou, C., Qi, Y.G., and Yu, J.S. (2017). Enhancement of Förster energy transfer from thermally activated delayed fluorophores layer to ultrathin phosphor layer for high color stability in non-doped hybrid white organic light-emitting devices. *Chin. Phys. B* 26, 047302.

Wang, Z.Q., Liu, Z.M., Zhang, H., Zhao, B., Chen, L.Q., Xue, L., Wang, H., and Li, W.L. (2018). Highly efficient and spectra stable warm white organic light-emitting diodes by the application of exciplex as the excitons adjustment layer. *Org. Electron.* 62, 157–162.

Wang, B.Q., Kou, Z.Q., Tang, Y., Yang, F.Y., Fu, X.E., and Yuan, Q.S. (2019a). High CRI and stable spectra white organic light-emitting diodes with double doped blue emission layers and multiple ultrathin phosphorescent emission layers by adjusting the thickness of spacer layer. *Org. Electron.* 70, 149–154.

Wang, Z.Q., Wang, C., Zhang, H., Liu, Z.M., Zhao, B., and Li, W.L. (2019b). The application of charge transfer host based exciplex and thermally activated delayed fluorescence materials in organic light-emitting diodes. *Org. Electron.* 66, 227–241.

Wang, Q., Tian, Q.S., Zhang, Y.L., Tang, X., and Liao, L.S. (2019c). High-efficiency organic light-emitting diodes with exciplex hosts. *J. Mater. Chem. C* 7, 11329–11360.

Wang, H., Dong, D., Lian, L., Zhu, F., Xu, D.Y., Wu, S.Y., and He, G.F. (2019d). High efficiency non-doped white organic light emitting diodes based on a bilayer interface-exciplex structure. *Phys. Status Solidi A-appl. Mat.* 216, 1900034.

Wang, B.Q., Kou, Z.Q., Yuan, Q.S., Fu, X.E., Fan, Z.T., and Zhou, A. (2020). Improving CRI of white phosphorescence organic light-emitting diodes by controlling exciton energy transfer in the planar heterojunction. *Org. Electron.* 78, 105617.

Wei, X., Yu, H.J., Cao, J., Jhun, C., and Chen, C.P. (2017). Efficient blue and white phosphorescent organic light-emitting diodes with a mixed host in

emission layer. *Mol. Cryst. Liquid Cryst.* 651, 108–117.

Wei, P.C., Zhang, D.D., and Duan, L. (2020). Modulation of Förster and Dexter interactions in single-emissive-layer all-fluorescent WOLEDs for improved efficiency and extended lifetime. *Adv. Funct. Mater.* 30, 1907083.

Wu, Z.B., and Ma, D.G. (2016). Recent advances in white organic light-emitting diodes. *Mater. Sci. Eng. R-rep.* 107, 1–42.

Wu, S., Li, S., Sun, Q., Huang, C., and Fung, M.K. (2016). Highly efficient white organic light-emitting diodes with ultrathin emissive layers and a spacer-free structure. *Sci. Rep.* 6, 1–8.

Wu, S.F., Li, S.H., Wang, Y.K., Huang, C.C., Sun, Q., Liang, J.J., Liao, L.S., and Fung, M.K. (2017). White organic LED with a luminous efficacy exceeding 100 lm W<sup>-1</sup> without light out-coupling enhancement techniques. *Adv. Funct. Mater.* 27, 1701314.

Wu, M.G., Wang, Z.J., Liu, Y.F., Qi, Y.G., and Yu, J.S. (2019). Non-doped phosphorescent organic light-emitting devices with an exciplex forming planar structure for efficiency enhancement. *Dyes Pigment* 164, 119–125.

Xiao, P., Huang, J.H., Yu, Y.C., Yuan, J., Luo, D.X., Liu, B.Q., and Liang, D. (2018). Recent advances of exciplex-based white organic light-emitting diodes. *Appl. Sci.* 8, 1449.

Xie, F.M., Zou, S.J., Li, Y.Q., Lu, L.Y., Yang, R., Zeng, X.Y., Zhang, G.H., Chen, J.D., and Tang, J.X. (2020). Management of delayed fluorophor-sensitized exciton harvesting for stable and efficient all-fluorescent white organic light-emitting diodes. *ACS Appl. Mater. Inter.* 12, 16736–16742.

Xu, T., Zhou, J.G., Huang, C.C., Zhang, L., Fung, M.K., Murtaza, I., Meng, H., and Liao, L.S. (2017). Highly simplified tandem organic light-emitting devices incorporating a green phosphorescence ultrathin emitter within a novel interface exciplex for high efficiency. *ACS Appl. Mater. Inter.* 9, 10955–10962.

Xu, T., Zhou, J.G., Fung, M.K., and Meng, H. (2018). Simplified efficient warm white tandem organic light-emitting devices by ultrathin emitters using energy transfer from exciplexes. *Org. Electron.* 63, 369–375.

Xue, Q., Xie, G.H., Liu, S.Y., Chen, P., Zhao, Y., and Liu, S.Y. (2014). Distinguishing triplet energy transfer and trap-assisted recombination in multicolor organic light-emitting diode with an ultrathin phosphorescent emissive layer. *J. Appl. Phys.* 115, 114504.

Xue, K.W., Han, G.G., Duan, Y., Chen, P., Yang, Y.Q., Yang, D., Duan, Y.H., Wang, X., and Zhao, Y. (2015a). Doping-free orange and white phosphorescent organic light-emitting diodes with ultra-simply structure and excellent color stability. *Org. Electron.* 18, 84–88.

Xue, K.W., Sheng, R., Chen, B.Y., Duan, Y., Chen, P., Yang, Y.Q., Wang, X., Duan, Y.H., and Zhao, Y. (2015b). Improved performance for white phosphorescent organic light-emitting diodes utilizing an orange ultrathin non-doped emission layer. *RSC Adv.* 5, 39097–39102.

Xue, K.W., Sheng, R., Duan, Y., Chen, P., Chen, B.Y., Wang, X., Duan, Y.H., and Zhao, Y. (2015c). Efficient non-doped monochrome and white phosphorescent organic light-emitting diodes based on ultrathin emissive layers. *Org. Electron.* 26, 451–457.

Yang, X.H., and Jabbour, G.E. (2013). Efficient light emitting devices based on phosphorescent partially doped emissive layers. *J. Mater. Chem. C* 1, 4663–4666.

Yang, X.L., Zhou, G.L., and Wong, W.Y. (2015). Functionalization of phosphorescent emitters and their host materials by main-group elements for phosphorescent organic light-emitting devices. *Chem. Soc. Rev.* 44, 8484–8575.

Yang, F.Y., Kou, Z.Q., Yang, L.P., and Tang, Y. (2018). Influence of the hole transport layer on spectral stability in the white phosphorescent organic light emitting diode with non-doped structure. *Opt. Mater.* 82, 130–134.

Yao, J.W., Liu, W., Lin, C.W., Sun, Q., Dai, Y.F., Qiao, X.F., Yang, D.Z., Chen, J.S., and Ma, D.G. (2021). High efficiency and long lifetime fluorescent white organic light-emitting diodes by phosphor sensitization to strategically manage singlet and triplet excitons. *J. Mater. Chem. C* 9, 3626–3634.

Yin, Y.M., Yu, J., Cao, H.T., Zhang, L.T., Sun, H.Z., and Xie, W.F. (2014). Efficient non-doped phosphorescent orange, blue and white organic light-emitting devices. *Sci. Rep.* 4, 1–7.

Yin, Y.M., Ali, M.U., Xie, W.F., Yang, H., and Meng, H. (2019). Evolution of white organic light-emitting devices: from academic research to lighting and display applications. *Mater. Chem. Front.* 3, 970–1031.

Ying, S.A., Yao, J.W., Chen, Y.W., and Ma, D.G. (2018a). High efficiency (~ 100 lm W<sup>-1</sup>) hybrid WOLEDs by simply introducing ultrathin non-doped phosphorescent emitters in a blue exciplex host. *J. Mater. Chem. C* 6, 7070–7076.

Ying, S.A., Yang, D.Z., Qiao, X.F., Dai, Y.F., Sun, Q., Chen, J.S., Ahamad, T., Alshehri, S.M., and Ma, D.G. (2018b). Improvement of efficiency and its roll-off at high brightness in white organic light-emitting diodes by strategically managing triplet excitons in the emission layer. *J. Mater. Chem. C* 6, 10793–10803.

Ying, S., Wu, Y.B., Sun, Q., Dai, Y.F., Yang, D.Z., Qiao, X.F., Chen, J.S., and Ma, D.G. (2019). High efficiency color-tunable organic light-emitting diodes with ultra-thin emissive layers in blue phosphor doped exciplex. *Appl. Phys. Lett.* 114, 033501.

Ying, S.A., Zhang, S., Yao, J.W., Dai, Y.F., Sun, Q., Yang, D.Z., Qiao, X.F., Chen, J.S., and Ma, D.G. (2020a). High-performance white organic light-emitting diodes with doping-free device architecture based on the exciton adjusting interfacial exciplex. *J. Mater. Chem. C* 8, 7019–7025.

Ying, S., Chen, Y.W., Yao, J.W., Sun, Q., Dai, Y.F., Yang, D.Z., Qiao, X.F., Chen, J.S., and Ma, D.G. (2020b). High efficiency doping-free warm-white organic light-emitting diodes with strategic tuning of radiative excitons by combining interfacial exciplex with multi-ultrathin emissive layers. *Org. Electron.* 85, 105876.

- Yu, J.S., Zhang, W., Wen, W., Lin, H., and Jiang, Y.D. (2011). Film thickness influence of dual iridium complex ultrathin layers on the performance of nondoped white organic light-emitting diodes. *Displays* 32, 87–91.
- Yu, H.J., Dai, X.D., Yao, F.N., Wei, X., Cao, J., and Jhun, C. (2018). Efficient white phosphorescent organic light-emitting diodes using ultrathin emissive layers (< 1 nm). *Sci. Rep.* 8, 1–8.
- Zhang, B.H., and Xie, Z.Y. (2019). Recent applications of interfacial exciplex as ideal host of power-efficient oleds. *Front. Chem.* 7, 306.
- Zhang, T.M., Shi, C.S., Zhao, C.Y., Wu, Z.B., Sun, N., Chen, J.S., Xie, Z.Y., and Ma, D.G. (2017a). High efficiency phosphorescent white organic light-emitting diodes with low efficiency roll-off achieved by strategic exciton management based on simple ultrathin emitting layer structures. *J. Mater. Chem. C* 5, 12833–12838.
- Zhang, H., Yang, X., Cheng, J., Li, D., Chen, H., Yu, J.S., and Li, L. (2017b). Enhanced color stability for white organic light-emitting diodes based on dual ultra-thin emitting layer. *Org. Electron.* 50, 147–152.
- Zhang, X.W., Zhang, M.K., Liu, M.J., Chen, Y.H., Wang, J., Zhang, X.L., Zhang, J.J., Lai, W.Y., and Huang, W. (2018a). Highly efficient tandem organic light-emitting devices adopting a nondoped charge-generation unit and ultrathin emitting layers. *Org. Electron.* 53, 353–360.
- Zhang, T.M., Shi, C.S., Zhao, C.Y., Wu, Z.B., Chen, J.S., Xie, Z.Y., and Ma, D.G. (2018b). Extremely low roll-off and high efficiency achieved by strategic exciton management in organic light-emitting diodes with simple ultrathin emitting layer structure. *ACS Appl. Mater. Inter.* 10, 8148–8154.
- Zhang, D.D., Song, X.Z., Cai, M.H., and Duan, L. (2018c). Blocking energy-loss pathways for ideal fluorescent organic light-emitting diodes with thermally activated delayed fluorescent sensitizers. *Adv. Mater.* 30, 1705250.
- Zhang, G.H., Xie, F.M., Wu, K., Li, Y.Q., Xie, G., Zou, S.J., Shen, Y., Zhao, X., Yang, C.L., and Tang, J.X. (2020). High-efficiency white organic light-emitting diodes based on all nondoped thermally activated delayed fluorescence emitters. *Adv. Mater. Inter.* 7, 1901758.
- Zhang, T.M., Yao, J.W., Zhang, S., Xiao, S., Liu, W., Wu, Z.B., and Ma, D.G. (2021). Highly efficient and low efficiency roll-off organic light-emitting diodes with double-exciplex forming co-hosts. *J. Mater. Chem. C* 9, 6062–6067.
- Zhang, T.M., Shi, C.S., Sun, N., Wu, Z.B., and Ma, D.G. (2021b). Simplified and high-efficiency warm/cold phosphorescent white organic light-emitting diodes based on interfacial exciplex co-host. *Org. Electron.* 92, 106123.
- Zhang, M., Zheng, C.J., Lin, H., and Tao, S.L. (2021c). Thermally activated delayed fluorescence exciplex emitters for high-performance organic light-emitting diodes. *Mater. Horizons* 8, 401–425.
- Zhao, Y.B., Chen, J.S., and Ma, D.G. (2011). Realization of high efficiency orange and white organic light emitting diodes by introducing an ultra-thin undoped orange emitting layer. *Appl. Phys. Lett.* 99, 226.
- Zhao, Y.B., Chen, J.S., and Ma, D.G. (2013a). Ultrathin nondoped emissive layers for efficient and simple monochrome and white organic light-emitting diodes. *ACS Appl. Mater. Inter.* 5, 965–971.
- Zhao, J., Yu, J.S., Wang, X., and Zhang, L. (2013b). Effect of two yellow delta-emitting layers on device performance of phosphorescent white organic light-emitting devices. *Solid-state Electron* 81, 63–67.
- Zhao, F.C., Zhu, L.P., Liu, Y.P., Wang, Y., and Ma, D.G. (2015). Doping-free hybrid white organic light-emitting diodes with fluorescent blue, phosphorescent green and red emission layers. *Org. Electron.* 27, 207–211.
- Zhao, J., Wang, Z.J., Wang, R., Chi, Z.G., and Yu, J.S. (2017). Hybrid white organic light-emitting devices consisting of a non-doped thermally activated delayed fluorescent emitter and an ultrathin phosphorescent emitter. *J. Lumines.* 184, 287–292.
- Zhao, C.Y., Zhang, T.M., Chen, J.S., Yan, D.H., and Ma, D.G. (2018a). High-performance hybrid white organic light-emitting diodes with simple emitting structures and low efficiency roll-off based on blue thermally activated delayed fluorescence emitters with bipolar transport characteristics. *J. Mater. Chem. C* 6, 9510–9516.
- Zhao, B., Zhang, H., Wang, Z.Q., Miao, Y.Q., Wang, Z.Q., Li, J., Wang, H., Hao, Y.Y., and Li, W.L. (2018b). Non-doped white organic light-emitting diodes with superior efficiency/color stability by employing ultra-thin phosphorescent emitters. *J. Mater. Chem. C* 6, 4250–4256.
- Zhao, C.Y., Yan, D.H., Ahamad, T., Alshehri, S.M., and Ma, D.G. (2019). High efficiency and low roll-off hybrid white organic light emitting diodes by strategically introducing multi-ultrathin phosphorescent layers in blue exciplex emitter. *J. Appl. Phys.* 125, 045501.
- Zhou, J., Kou, Z.Q., Wang, L.J., Wang, B.Q., Chen, X., Sun, X., and Zheng, Z.X. (2021). Realizing high-performance color-tunable WOLED by adjusting the recombination zone and energy distribution in the emitting layer. *J. Phys. D-appl. Phys.* 54, 265107.
- Zhu, L.P., Zhao, Y.B., Zhang, H.M., Chen, J.S., and Ma, D.G. (2014). Using an ultra-thin non-doped orange emission layer to realize high efficiency white organic light-emitting diodes with low efficiency roll-off. *J. Appl. Phys.* 115, 244512.
- Zhu, Y.K., Zhong, J., Lei, S.Y., Chen, H., Shao, S.S., and Lin, Y. (2017). High-efficiency organic light-emitting diodes based on ultrathin blue phosphorescent modification layer. *Chin. Phys. B* 26, 087302.
- Zou, S.J., Zeng, X.Y., Li, Y.Q., and Tang, J.X. (2021). The strategies for high-performance single-emissive-layer white organic light-emitting diodes. *Laser Photon. Rev.* 15, 2000474.